GCAGS JOURNAL
A Publication of the Gulf Coast Association of Geological Societies
www.gcags.org

Eagle Ford–A Depositional Setting and Processes in Southwestern Texas: An Example of Deeper-Water, Below-Storm-Wave-Base Carbonate Sedimentation on a Drowned Shelf

Robert G. Loucks

Bureau of Economic Geology, Jackson School of Geosciences, University of Texas at Austin, University Station, Box X, Austin, Texas 78713–8924, U.S.A.

ABSTRACT

The Upper Cretaceous, lowermost Eagle Ford Group (Eagle Ford–A member), southwestern Texas, displays an interesting array of depositional features interpreted to have been deposited on a deeper-water, inclined, drowned shelf below storm-wave base. The unit is landward of the Lower Cretaceous paleo–Stuart City shelf margin. Strata are composed of only deeper-water biotas, including coccoliths, globigerinids, calcispheres, pelagic crinoid fragments, inoceramid fragments, small ammonites, and rare radiolarians. No evidence of bioturbation is present, and argillaceous mudstones contain elevated TOC (total organic carbon) (up to 2 wt%). Sedimentary features include gravity flows (concentrated and surge-like flows), low-density turbidites, hummocky cross-stratification-like bedding, swaley cross-stratification-like bedding, bottom-current ripples and megaripples, load features, regional (tens of miles) slump and slide units, and regional-scale volcanic ash beds.

Biological assemblage and depositional features all support a deeper-water setting below storm-wave base, where bottom conditions were anoxic. Lack of any nearshore, shallow-water biotas and an overwhelming abundance of open-marine biotas support deposition distal of any shoreline. Planktic biotas support deeper-water deposition far out on a drowned shelf. Total absence of bioturbation and elevated TOC is strong evidence of anoxic bottom conditions below storm-wave base. Hydrodynamic sedimentary features, such as turbidites, hummocky cross-stratification-like bedding, swaley cross-stratification-like bedding, bottom-current ripples and megaripples, and load features can all be related to deeper-water, below-storm-wave-base processes.

Objections to a below-storm-wave-base depositional setting have been presented by authors who interpret hummocky cross-stratification-like bedding as storm-wave-related, hummocky cross-stratification. These researchers have taken this feature as irrefutable evidence of deposition above storm-wave base. However, other researchers have documented hummocky-like cross-stratification in deepwater carbonates and attribute the process of formation not to storms, but to deeper-water processes. Other depositional features, such as debrites, turbidites, bottom-current ripples and megaripples, load features, regional (tens of miles) slump and slide units, and regional-scale volcanic ash beds, are more consistent with deeper-water deposition dominated by gravity flows, mass movement, and suspension deposition. Therefore, when all evidence is weighed and considered, a deeper-water, below-storm-wave-base setting is the logical interpretation for the depositional setting of Eagle Ford–A strata.

INTRODUCTION

The Upper Cretaceous (Cenomanian) lowermost Eagle Ford member (Eagle Ford–A, which is equivalent to the lowermost Boquillas member of Donovan and Staerker [2010] and Donovan et al. [2012]) (Fig. 1) is composed of carbonate strata that were deposited in southwestern Texas on the drowned Lower Cretaceous shelf (Fig. 2). This carbonate-dominated section is notable in its abundance of sedimentary structures produced by both hydrodynamic processes and synsedimentary deformational mechanisms; it is therefore an opportunity to investigate processes and products of fine-grained carbonate sedimentation (argillaceous chalk).

A major goal of this investigation is to present a sedimentological interpretation of the Eagle Ford–A section that is based on integration of regional setting, biotas, hydrodynamic features, and syndepositional soft-sediment deformation. Specific objectives include (1) defining the regional setting of the study area,

Manuscript received March 21, 2018; revised manuscript received May 7, 2018; manuscript accepted May 9, 2018.

GCAGS Journal, v. 7 (2018), p. 59–78.

Figure 1. Upper Cretaceous stratigraphic section in the study area. Time intervals based on Gradstein et al. (2012) and stratigraphy based on Donovan et al. (2012).

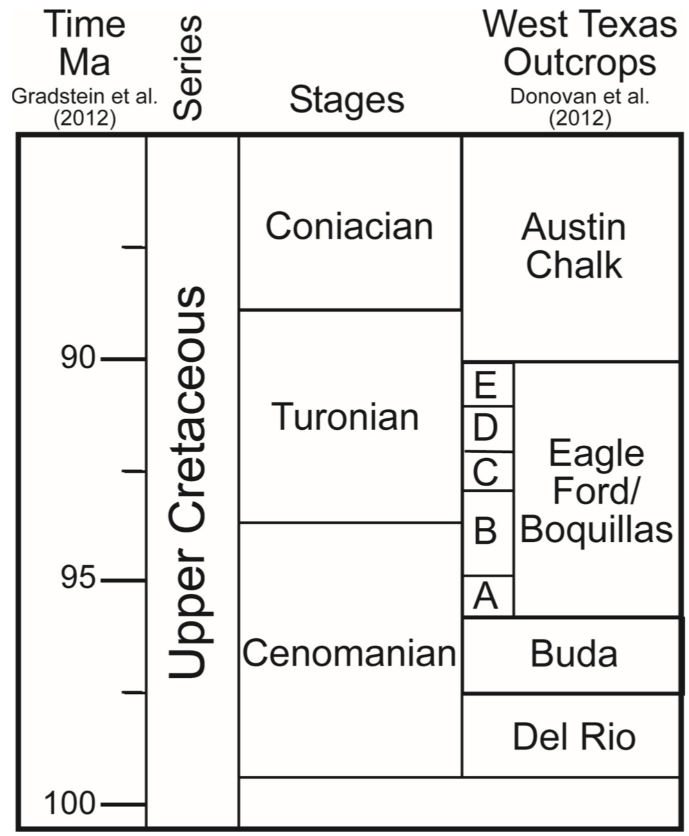

Figure 2. Aerial map of the Eagle Ford shelf (from Pierce et al., 2016, reproduced with permission of the Gulf Coast Association of Geological Societies).

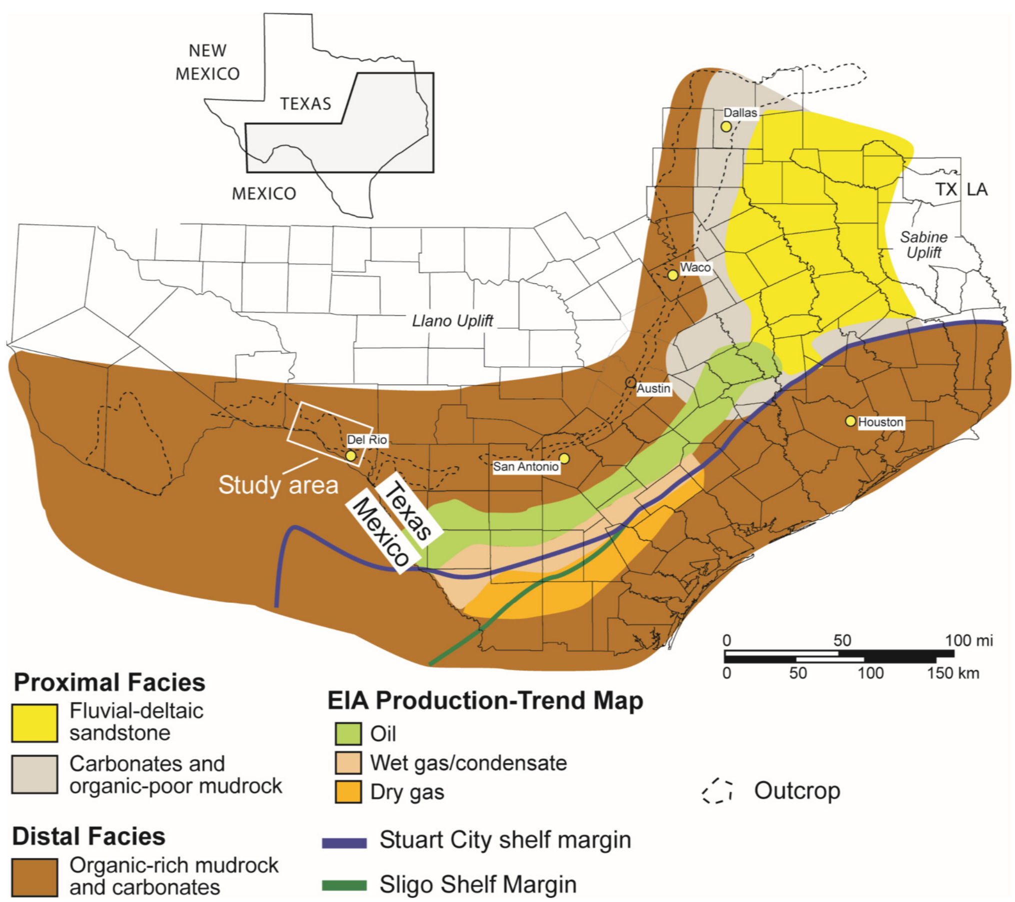

(2) reviewing Eagle Ford–A biotas and establishing their living environments and methods of accumulation, (3) presenting and interpreting hydrodynamic features and synsedimentary deformational structures, (4) defining regional intrastratal architecture of the Eagle Ford–A section, and (5) discussing the depositional setting of Eagle Ford–A strata through integrating both biotas and sedimentary features.

This investigation of the lower Eagle Ford section should be of interest because it will assist in an understanding of the regional depositional architecture of the complete Eagle Ford Group. Also, investigation of this carbonate-rich unit will add to our understanding of deeper-water carbonate sedimentary features and associated deformation and deformational processes, as well as the depositional setting of where they form.

DATA AND METHODS

A series of fresh roadcuts along U.S. Highway 90 west of Del Rio, Texas, and along U.S. Highway 277 north of Del Rio (Fig. 3), contains excellent exposures of the Eagle Ford–A section, and several of these roadcuts show its entire 25- to 30-ft (7.6- to 9.1-m) thick section. Nearly all roadcuts display the lower contact of the Eagle Ford–A with the Buda Formation, but not the upper contact with the Eagle Ford–B section. Roadcuts along Highway 90 are aligned generally along strike to slightly oblique to strike, and roadcuts along Highway 277 are aligned generally along dip.

Photographs of roadcuts (Fig. 4) were collected to produce continuous lateral sections that were analyzed for depositional packages and structures. Some roadcuts, more than several thousand feet long, provided data on short-distance continuity and heterogeneity. Also, correlation of widely-spaced roadcuts along the highway provided data on possible larger-scale, regional depositional packages.

At several roadcuts, rock slabs were collected for analysis of sedimentary textures, fabrics, and finer-scale structures. The rock samples were slabbed, etched with 10% HCl, and described using a binocular microscope. Selected slabs were sampled for thin sections, X–ray diffraction (XRD) analysis, and total organic carbon (TOC).

Data presented in this investigation are compared with Eagle Ford–A data collected from the same general area by other investigators. Authors who have investigated this Eagle Ford–A area include Treviño (1988), Miller (1990), Lock and Peschier (2006), Lock et al. (2007, 2010a, 2010b), Donovan and Staerker (2010), Donovan et al. (2012, 2015), Denne et al. (2014), Wehner et al. (2015), and Minisini et al. (2018).

STRATIGRAPHY AND GENERAL DEPOSITONAL SETTING

Stratigraphy

The Eagle Ford Group is Late Cretaceous in age (early Cenomanian to late Turonian) (e.g., Donovan et al., 2015; Eldrett et al., 2015) (Fig. 1) and has been divided into different units by different authors. In the present study, the section investigated is the basal Eagle Ford section, which rests on the Buda Formation (Fig. 1). Donovan and Staerker (2010, p. 871) and Donovan et al. (2012) informally named the lowermost unit in the Eagle Ford Group in the Del Rio area "the Eagle Ford–A unit" (Fig. 1). Note that, in the study area, Eagle Ford and Boquillas sections are largely age equivalent. The section has been designated the Eagle Ford Group east of the Pecos River and the Boquillas Formation west of the Pecos River (e.g., Lock et al., 2010b). For simplicity, in this investigation, the section under study is referred to as "Eagle Ford–A," even though roadcuts on both sides of the Pecos River are within the dataset.

The Eagle Ford–A section is in erosional contact with the underlying lower Cenomanian Buda Limestone below. Buda strata were deposited as a chalk on the drowned Lower Cretaceous shelf following transgression of the siliciclastic-dominated Del Rio section (Fig. 1). The contact is sharp but irregular and has an undulatory surface with relief of up to 0.65 ft (20 cm). The top of the Buda surface appears to have been well lithified, showing no evidence of subaerial weathering or submarine hardground formation; however, some authors have suggested that the top of the Buda has been karsted (e.g., Lock and Peschier, 2006). The uppermost Buda section has been highly burrowed by large *Thalassinoides*. The material within the

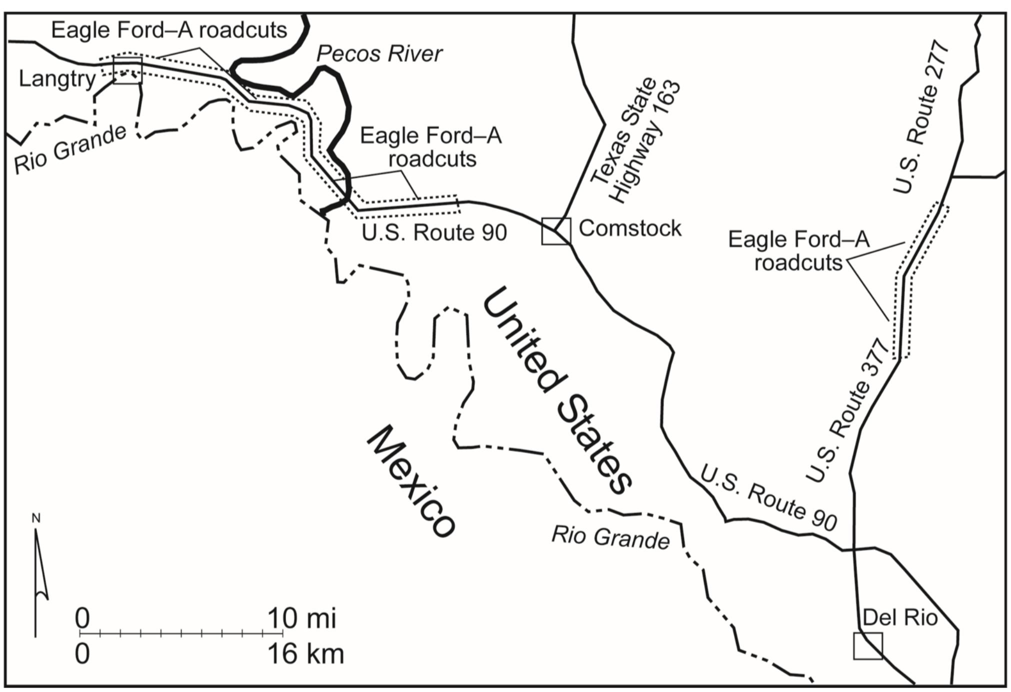

Figure 3. Map showing areas (dashed outlines) of Eagle Ford–A strata roadcuts investigated.

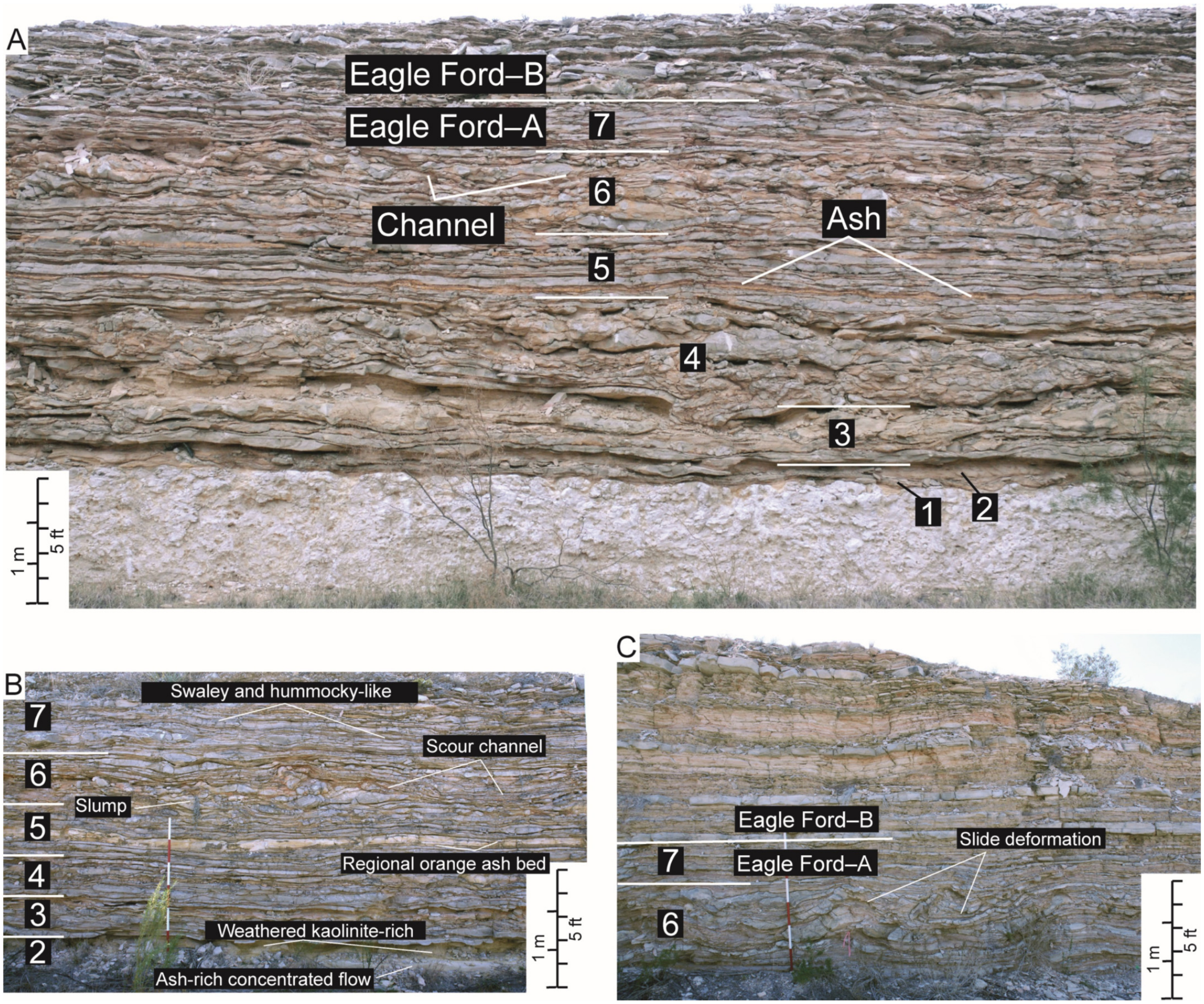

Figure 4. Examples of internal architecture of Eagle Ford–A strata. Eagle Ford–A section is informally divided into seven units somewhat correlatable over study area. (A) Buda through base of Eagle Ford–B interval. All seven Eagle Ford–A units present. (B) Eagle Ford–A units 2 through 7 present. Regional "orange" ash bed in unit 5. (C) Contact of Eagle Ford–A section with Eagle Ford–B section. Upper part of Eagle Ford–A with soft-sediment, slide-deformation features.

burrows is not similar to Eagle Ford sediment above, suggesting that the burrows were not open at the time of lower Eagle Ford deposition. Also, several lithoclasts of Buda lithology were noted in lower Eagle Ford–A deposits. Denne et al. (2014) suggested a 2-million-yr break between Buda and Eagle Ford sections.

The Eagle Ford–A is gradational into the overlying Eagle Ford–B. The transition ranges from wavy, discontinuous bedding to more continuous bedding (Figs. 4A and 4C). TOC increases from approximately 2% to as much as 6 to 7%. Several authors have interpreted this transition to be related to a deepening event in the middle Eagle Ford section (e.g., Donovan and Staerker, 2010; Frébourg et al., 2016).

The Eagle Ford–A section discussed in this investigation appears to be present only in this southwestern area of Texas and possibly Mexico (Lock et al., 2007, 2010b; Donovan and Staerker, 2010). No core data are available to document the eastern pinch-out of the Eagle Ford–A or how it correlates with the Eagle Ford section in South Texas; however, a wireline-log cross section presented in Lock et al. (2010b, their figure 7) shows the Eagle Ford–A section pinching out to the southeast.

General Depositional Setting

The general depositional setting of Eagle Ford–A strata was on the drowned Lower Cretaceous shelf (Fig. 2). Following deposition of upper Albian strata, which included the shelf-edge Stuart Reef Trend and the platform-interior Devils River section (Phelps et al., 2013), a major unconformity developed, followed by a second-order transgression that flooded the shelf (Phelps et al., 2013). Restricted, shallow-water Del Rio siliciclastics were the initial deposits on the Lower Cretaceous unconformity in the study area (Lock et al., 2009, 2013) (Fig. 1), and the deeper-water Buda chalk transgressed the Del Rio siliciclastics. The Buda Formation is a moderate-depth, open-marine chalk with major components of coccoliths, globigerinids, and calcispheres (data collected by senior author). Some cephalopods were noted.

A minor abundance of benthic biotas is present, including foraminifers, bivalves, gastropods, and rare corals. Strata are highly bioturbated by *Thalassinoides*, indicating well-oxygenated bottom waters and sediments.

Deposition of lower Eagle Ford–A strata reflects a major change in environmental conditions from the Buda interval. As will be discussed in more detail in the next section, the biota of lower Eagle Ford–A strata is planktic in origin (no benthic foraminifers) [this study; Lock and Peschier, 2006; Lowery et al., 2014] except for inoceramid bivalves) and no bioturbation is noted (this study; Lock and Peschier, 2006), whereas Buda strata contain a combination of benthic and planktic biotas and were intensely bioturbated (data collected by author). Also, TOC in the Buda section is present in trace amounts (less than 0.3 wt%), as compared with lower Eagle Ford–A strata, where it is up to 2.0 wt% (this study; Treviño, 1988; Donovan et. al., 2012). This abrupt change in environmental conditions suggests a more restricted environment for Eagle Ford–A strata than in Buda strata. The oceanic anoxic event 2 (OAE–2) did not develop until later, during middle Eagle Ford time (Donovan et. al., 2012; Eldrett et al., 2015; Alnahwi et al., in press), so anoxia in Eagle Ford–A strata is not related to this event. The cause for the change to dysaerobic/anaerobic conditions is debatable, but a stratified water column may have developed in Eagle Ford–A time that did not exist in Buda time.

Paleotopography may have been associated with the relict Stuart City shelf-margin buildup, partly barring the basin and producing restricted conditions (Alnahwi et al., in press). Buda chalk deposition was not in a restricted environment, which may be explained by sea level during Buda time being high enough that circulation across the paleoshelf edge was adequate to keep the drowned shelf oxygenated. During Eagle Ford–A time, waters on the drowned shelf may not have been as deep as during Buda time, and the proposed silled rim aided in development of a stratified water column. However, waters had to be deep enough to restrict mixing of shallower, oxygen-rich waters with deeper, oxygen-depleted waters by large storms (i.e., water depth was greater than storm-wave base).

At the time of Eagle Ford–A deposition, the Western Interior Seaway was not connected to the paleo–Gulf of Mexico (as postulated by reconstructed paleogeographic maps by Blakely [2018]), which would have restricted large-scale, bottom-current flow of colder waters in the north into the area of study. Therefore, restriction seen in Eagle Ford–A strata may have been related to the paleotopography of the relic Stuart City shelf margin to the south and with no connection to the Western Interior Seaway to the north.

The drowned Eagle Ford–A platform must have had a slight seaward dip because soft-sediment slumps and slides are common. Hance (2003) collected data on Holocene and Pleistocene slumps and slides and concluded that a slope of less than 0.5° can produce these features. He noted a correlation between more aerially, widely-distributed slides with lower angles of slope. Some slopes of less than 1° produced slides covering 9600 mi^2 (25,000 km^2), as noted in his study. Therefore, the Eagle Ford–A drowned platform would not have needed much of a slope for mass-movement-associated slumps and slides.

BIOTA, LITHOFACIES, SEDIMENTARY FEATURES, AND SOFT-SEDIMENT DEFORMATION IN THE EAGLE FORD–A UNIT

Introduction

Biota and sedimentary features are introduced, described, and discussed in this section. Some sedimentary features are controversial as to their origin, so evidence is presented to best interpret how and where they formed. A review of the biota that produced sediments of Eagle Ford–A strata is essential because the biota provides important limitations on how and where sediments were deposited. Overall, to establish depositional setting, both the biota and sedimentary structures need to be described and analyzed.

A significant concept in developing an understanding of depositional setting and associated sedimentary features of Eagle Ford–A strata is storm-wave base and its relationship to sedimentary processes. Therefore, as an introduction to this section, the concept of storm-wave base is discussed. Many sedimentary structures observed in the Eagle Ford–A are debatable as whether they are related to storm-produced gravity waves or to unidirectional currents deeper in the water column.

Storm-Wave Base

Because depositional sedimentary structures are related to physical properties of sediments and hydrodynamic processes and not directly to water depth (Peters and Loss, 2012), it is more insightful to relate depositional processes to its position above or below storm-wave base, rather than to water depth. Storm-wave base is defined as the greatest depth at which surface-gravity waves are able to entrain sediment. Reading and Collinson (1996) determined this depth to be less than or equal to approximately one half the wavelength of surface waves. Peters and Loss (2012, p. 513) maintained that storm-wave base is not an exact water depth but "a probability-based profile, with gradational boundaries that are defined by the probability of wave encounter and the formation and preservation of discrete sedimentary structures that reflect sediment supply and hydrodynamics." As an example of range of general depths to storm-wave base, Reading and Collinson (1996) noted that in offshore Florida, the estimated 10% probability of wave encounter on bottom sediments would be approximately 150 ft (50 m) on the Gulf of Mexico side and 300 ft (100 m) on the open Atlantic side.

Storm-wave base is an important boundary for hydrodynamic processes. Above storm-wave base, oscillatory or oscillatory-combined flow is common, whereas unidirectional flow is dominant below storm-wave base. Some oscillatory or oscillatory-combined flow processes are, however, possible below storm-wave base. Pycnocline flow at the interface of fluids of different densities can generate internal waves that can impinge on bottom sediment below storm-wave base (e.g., Shanmugam, 2008; He et al., 2011). Prave and Duke (1990) and Mulder and Alexander (2001) suggested that reverse-flow standing waves can reproduce oscillatory-like currents that form in the upper flow interface of turbidity currents. Also, as explained by Pickering and Hiscott (1985), Pantin and Leeder (1987), and Basilici et al. (2012), deepwater density currents, below storm-wave base, interacting with topography on the sea bottom can produce reserve currents, which, in turn, can produce undulating laminations and bidirectional cross-laminations. Oscillatory-like currents are therefore possible below storm-wave base, and structures associated with these currents should not be misinterpreted as above-storm-wave-base-produced features.

Also, to produce dysaerobic to anaerobic bottom conditions on a shelf, a stratified water column would appear to be necessary to allow stagnation. If bottom sediments were within storm-wave base, oxygen-poor water below would mix with oxygen-rich water above on a periodic basis. There is no rock evidence of such mixing in the Eagle Ford–A section.

A number of case histories have been presented in the literature to address whether sedimentation occurred above or below storm-wave base (e.g., Basilici et al., 2012). Most of these case histories were conducted on siliciclastic units in which sediments were sourced from land and transported to the area of deposition. Siliciclastic sediments themselves add little evidence relative to depositional setting, whereas biogenic carbonate sediments deposited in the Eagle Ford–A section were all formed in a marine environment. These carbonate sediments therefore carry with

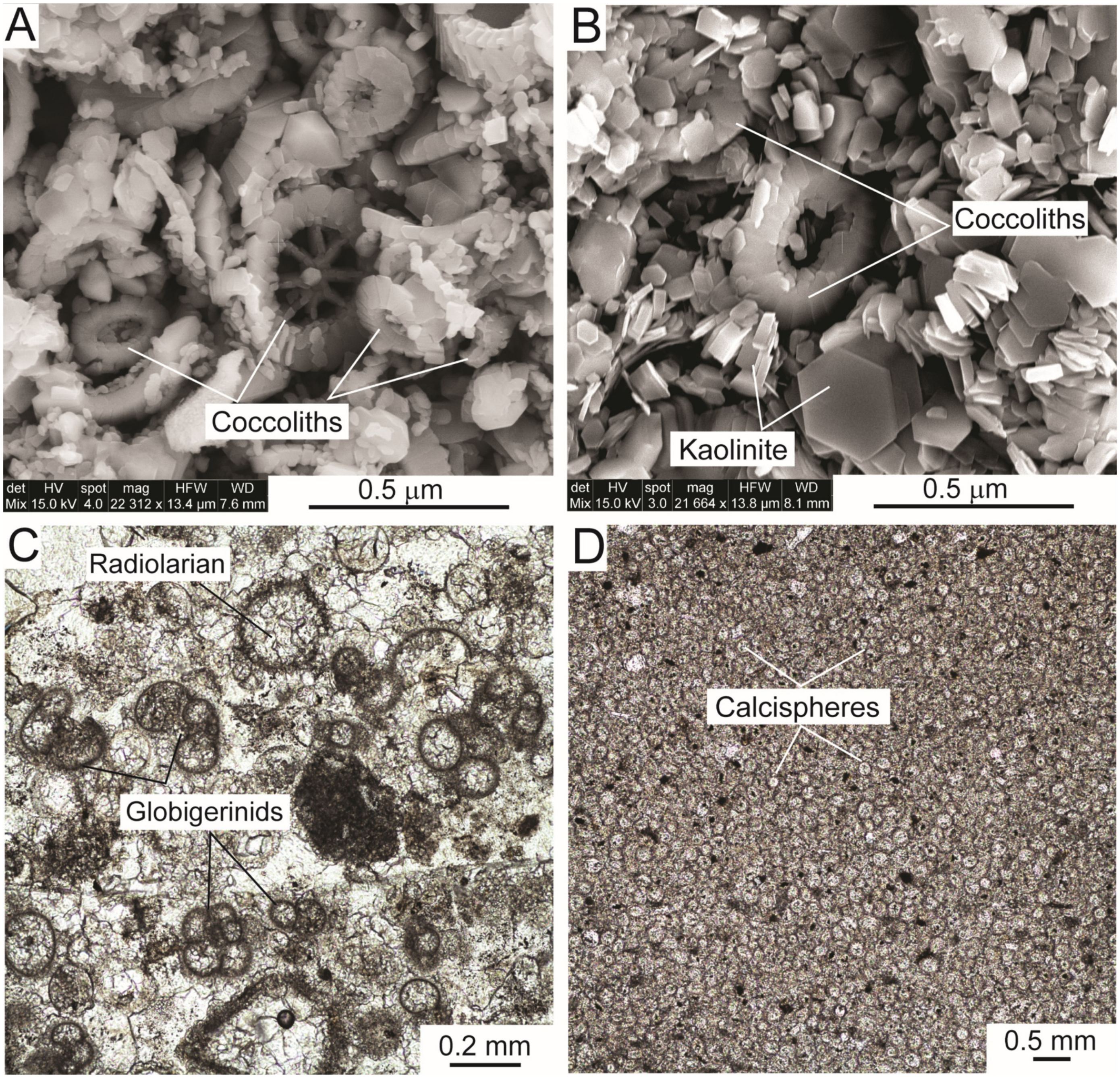

Figure 5. Examples of Eagle Ford–A textures and components. (A) SEM image of coccolith matrix. (B) Coccoliths in kaolinite-clay matrix. (C) Globigerinids in grainstone cemented by very-fine equant calcite. Radiolarian present. (D) Densely-packed calcispheres probably related to algal bloom.

them important evidence about the marine environment in which they originated and where they accumulated.

Biota and Bioturbation

The biota in lower Eagle Ford strata comprises predominately open-marine planktic flora and fauna and represents deposition in deeper water away from higher-energy areas. In this section, the biota is reviewed, and pertinent facts are given relative to living conditions of the biota and depositional setting. Figures 5 and 6 show thin-section examples of the biota from the Eagle Ford–A interval.

Coccolithophores

The most abundant grain type in Eagle Ford–A strata is fragments (coccoliths) of coccolithophores (Figs. 5A and 5B), which are marine, unicellular phytoplankton organisms (e.g., Guerreiro, 2013). Coccolithophores are photosynthesizers that are restricted to the photic zone, in warm, stratified, oligotrophic waters. They prefer still, nutrient-poor water and once they become established, they become dominant over other organisms (Earth Observatory, 2018). Guerreiro (2013) noted that most coccolithophore species dwell in the upper 165 to 260 ft (50 to 80 m) of the photic zone. He also noted that most species are photo-inhibited

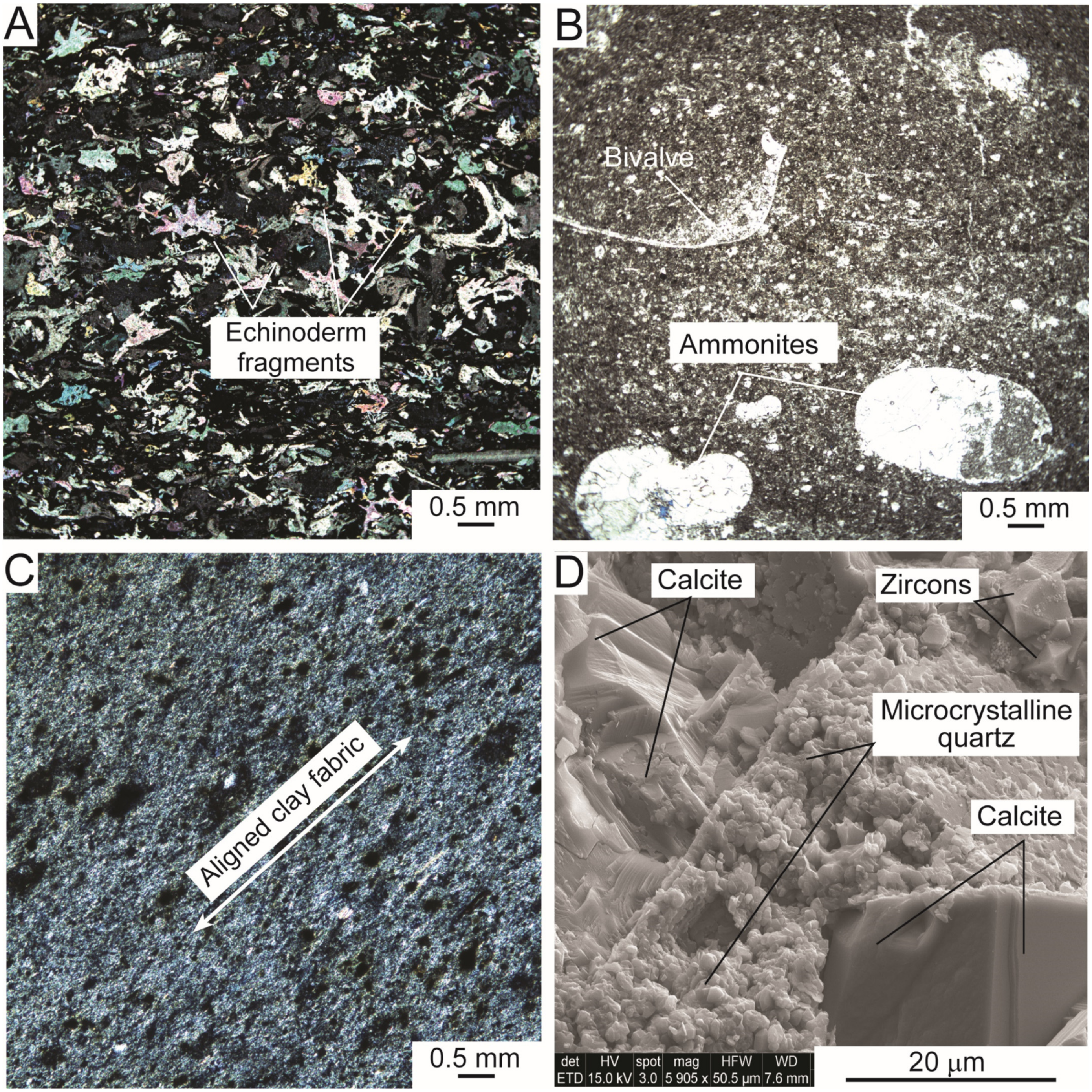

Figure 6. Examples of Eagle Ford–A textures and components. (A) Saccocomid grainstone. Cross-polarized light. (B) Ammonite-bearing packstone. (C) Altered volcanic ash composed of clay minerals. Thin section rotated 45° under cross-polarized light to emphasize alignment of clays. (D) SEM image of volcanic ash shown in C. Alteration products of the ash are kaolinite, calcite, and microcrystalline quartz. Several zircons are present.

near the surface. Many other species prefer to live in the lower photic zone between 325 and 650 ft (100 and 200 m).

Individual coccolithophores settle to the bottom slowly, but, as shown by several researchers (Roth, 1994; Steinmetz, 1994; Balch, 2004), most coccolithophores are transported through the water column as part of fast-sinking fecal pellets (Guerreiro, 2013) generated by grazing zooplankton or by aggregates of marine snow. Coccolithophores begin to break down into coccoliths and elements as they descend through the water column, as evidenced by collections in suspended-sediment-trap studies (e.g., Broerse et al., 2000; Ziveri et al., 2000a, 2000b). Coccoliths were found to be three to four orders of magnitude greater in abundance than coccolithophores in collected samples and these authors related this difference to the polysaccharide membrane that holds the coccolithophores together, which breaks down by digestion in herbivorous zooplankton. Roth (1994) suggested that metabolization by bacteria during transport to the seafloor also breaks down the polysaccharide membrane.

Scanning electron microscope (SEM)–based analysis of Eagle Ford–A samples shows that coccoliths and associated elements compose the matrix (Figs. 5A and 5B). These very-fine grains were and still are calcite, and the major diagenesis they have undergone is simple calcite overgrowth cementation. As this discussion of coccolithophores has suggested, coccolith-rich sediments support an open-marine, deeper-water setting, and, as noted by Guerreiro (2013, p. 30), "coccoliths will preferentially accumulate in fine-grained hemipelagic deposits that accumulate in more quiescent environments."

Planktic Foraminifers

Planktic foraminifers, including common globigerinids (Fig. 5C), are also abundant in the Eagle Ford–A, and they lived in the euphotic zone in a marine environment (e.g., Bé, 1960). Bé (1960) noted that most planktic foraminifers probably had symbiotic zooxanthellae, and through this symbiotic relationship they had a food source. Planktic foraminifers need light for photosynthesis, this requirement being critical in limiting planktic foraminifera to the upper 650 ft (200 m) of the water column and, generally, into the upper 330 ft (100 m). Boltovskov and Wright (1976) noted that planktic foraminifers avoid nearshore, shallow-water areas and prefer an open-marine environment. After death, planktic foraminifer tests settle to the sea bottom.

Note that in this discussion of foraminifers that no benthic foraminifers are observed in Eagle Ford–A strata. In modern shelf environments, benthic foraminifers are common in shallower waters above storm-wave base and decrease significantly as water depth and distance from shore increase (van der Zwann et al., 1990). Van der Zwann et al. (1990) attributed increases in abundance of planktic foraminifers to decreases in turbidity, which allowed primary production to increase. They noted that at increased water depths the nutrient chain and recycling loops are fully developed and planktic foraminifers can produce throughout the photic zone. Several plots were provided by van der Zwann et al. (1990) that show an increase in percent of planktic foraminifers with depth on seven modern shelves. On each shelf, some benthic foraminifers are present down to 1500 ft (500 m) (see their figure 2). Applying this reasoning to Eagle Ford–A strata, water depths must have been great, or some restriction occurred to have allowed development of a stratified water column. The total absence of benthic foraminifers therefore suggests deepwater sedimentation or anoxic bottom waters. Also, Williams (1963) found that sediment on the northern Yucatan platform near the shelf break (depths of ~450 ft [~140 m]) contains abundant planktic foraminifera but also contained 20 to 60% shallow-water-derived allochems. If the Eagle Ford–A sediments had been deposited within storm-wave base, some benthic foraminifers or other shallow-water allochems would be expected to be present. The total lack of benthic foraminifers, however, supports a deeper-water, drowned-platform environment that was a significant distance from shore.

Calcispheres

In Eagle Ford–A strata, calcispheres vary in abundance from common to extremely common (Fig. 5D). Classified as planktic, calcareous, dinoflagellate cysts, they lived in the shallower-water column in the photic zone (Vink, 2004). Flügel (2004) discovered that calcispheres are generally found in sediment in deep-shelf to slope sediment and less commonly in inner-shelf sediment. They are generally associated with coccolithophores, globigerinids, and other planktic organisms. Some samples as seen in thin section in Eagle Ford–A strata are nearly 100% calcispheres (Fig. 5D) and were probably associated with algal blooms. These allochems are found in abundance in only open-marine conditions and are deposited by suspension into low-energy, deeper-water environments.

Saccocomids

Several beds near the bottom of the Eagle Ford–A section have abundant saccocomid fragments (Fig. 6A). Saccocomids are pelagic or swimming crinoids that were common in the Late Cretaceous (e.g., Moore, 1967). They floated in the water column and were not attached or anchored to the sea bottom. The author has also noted saccocomid fragments from several deeper-water Albian South Texas shelf deposits.

Lock and Fife (2004) and Lock and Peschier (2006) also identified these echinoderm fragments in the Eagle Ford–A unit and have debated if these allochems are saccocomid (free floating crinoids) or ophiuroid (benthic brittle star) fragments. They noted that this distinction is important as ophiuroids lived on the bottom and saccocomids lived in the water column. Ophiuroids would need an oxygenated setting to live on the bottom. If the bottom was anoxic, they could be carried in by gravity flows (Lock and Peschier, 2006). However, if the fragments are ophiuroids and transported in from shallower-water areas by gravity flows, then other shallower-water biota should have also been carried in to the study area. This did not happen; therefore, the echinoid fragments are more likely saccocomids that lived in the offshore water column.

Cephalopods

Small ammonites that Hazzard (1959) classified as desmoceratids occur in Eagle Ford–A strata were noted at several locations in Eagle Ford–A strata, and in thin section they measure approximately 1.0 in (2.5 cm) in diameter (Fig. 6D). Ammonites are pelagic and can maneuver throughout the water column (Landman and Greyssant, 1993). Ammonites are generally restricted to deeper water—their association with coccolithophores, planktic foraminifers, and calcispheres supports this concept.

Radiolarians

Radiolarians are relatively rare in Eagle Ford–A strata (Fig. 5C), and examples viewed in this study have been replaced with calcite. Some examples have remnants of spines. These organisms are marine holoplanktonic protozoa that are free floating and drift along with water currents (MicrobeWik, 2018). Radiolarians can form symbiotic relationships with algae and dinoflagellates and occur throughout the water column from near surface to hundreds of feet in depth. In the present-day Gulf of Mexico, most radiolarians live in the upper 300 ft (90 m) of the water column, but some extend several thousand feet down (Casey et al., 1979). Leavesley et al. (1978) noted that radiolarians on the present-day South Texas shelf are indicative of open-marine conditions and become abundant with upwelling from the deeper open Gulf.

Inoceramids

Broken fragments of inoceramid bivalves are found scattered throughout the Eagle Ford–A section. They are common in other, deeper-water chalks (deposited below storm-wave base) of the Upper Cretaceous in Texas, such as the Buda Formation and the Austin Chalk Group. No whole specimens were noted. Inoceramids were flat and thin, which allowed them to live on soft, muddy bottoms without sinking into the mud. Large gill area allowed them to survive in oxygen-deficient waters (Boucot, 1990). These bivalves are the only bottom dwellers noted in Eagle Ford–A strata. The isolated, broken pieces suggest that the inoceramid fragments were emplaced by gravity flows.

Bioturbation

A significant observation about the strata of the Eagle Ford–A section is the complete lack of bioturbation (also observed by Lock and Peschier [2006]), and, because of this lack, sedimentary features are well preserved. Savrda and Bottjer (1989) found that benthic oxygenation levels are a critical factor in controlling life and activity of benthic organisms, especially in deeper-water, low-energy settings, so oxygenation levels control composition of the infaunal communities in marine-mud substrates. In turn, ichnofabrics in pelagic mudstones can function as a proxy indicator of the level of oxygenation of paleo-bottom-water conditions. Several authors (e.g., Ekdale and Mason, 1988; Bromley, 1990) have recognized that muddy sediments lacking trace fossils (abiotic) and displaying well-preserved sedimentary structures suggest dysaerobic to anaerobic bottom conditions.

Comment on Biota and Bioturbation

The predominance of a planktic biota, absence of all benthic biotas except inoceramids, absence of any trace fossils (no bioturbation), and raised levels of TOC (as high as 2 wt% as recorded by Treviño [1988] and Donovan et al. [2012]) signify that bottom-water conditions during early Eagle Ford deposition were dysaerobic to anaerobic. This is the same conclusion as by Lock and Fife (2004). With aerobic conditions near the sea surface and dysaerobic to anaerobic conditions at the sea bottom, a stratified water column must have existed. Therefore, to maintain a well-stratified water column, intense storm-wave action probably did not have much, if any, effect on bottom sediments.

Lithofacies

Three general lithofacies are in the Eagle Ford–A section in the study area: (1) planktic lime wackestones to grainstones having various amounts of argillaceous material, (2) calcareous argillaceous siliciclastic mudstones, and (3) altered volcanic ash beds.

Planktic Lime Packstone to Grainstone Lithofacies

Amount or absence of lime mud defines the texture of this lithofacies, and Eagle Ford–A mud is predominantly composed of coccolith elements and lesser amounts of clay minerals (Figs. 5A and 5B). Transfer of sediments to the sea bottom was by direct suspension (planktic ooze and volcanic ash) or from resedimentation of previously-deposited planktic ooze or volcanic ash. The overall biota is therefore similar in packstones and grainstones; however, the ratio of individual organism groups therein varies.

Argillaceous Siliciclastic Mudstone Lithofacies

Interbedded siliciclastic mudstones are thin and dominated by clay minerals. Several XRD analyses by Treviño (1988) and this investigation indicate that the clay is a combination of smectite, illite, and kaolinite. Some clay minerals, such as kaolinite and smectite, are most likely an alteration product of volcanic ash (Pierce et al., 2016). Carbonate content is as high as 40% and reflects a mixture of clay minerals with planktic organisms. Some of these mudstones may be Bouma Td mud drapes (based on position in turbidite units; discussed below) deposited by waning flows, or they could be altered volcanic ash beds.

Volcanic Ash Lithofacies

Volcanic ash beds are common in Eagle Ford Group strata (e.g., Pierce et al., 2016), and the Eagle Ford–A contains several prominent ash beds, with one orange-colored ash bed extending for more than 20 mi (32 km) (Fig. 4B). This ash bed was traced out by Lock and Peschier (2006) and described as a turbidite. Beds that are interpreted as weathered volcanic ash (Fig. 6C) consist of mixtures of microcrystalline quartz, calcite, dolomite, and clay minerals (Figs. 6C and 6D). A few larger grains of quartz are present in several samples. Dolomite rhombs commonly have hollow centers, which may have been calcite rich, as shown by SEM analysis. Because dolomite in the Eagle Ford–A is predominantly in weathered ash beds, the dolomite is assumed to be related to diagenesis of the volcanic ash. Most quartz grains or crystals are not readily visible in thin section, but SEM analysis shows that quartz is microcrystalline in the form of irregular spheres and crystals ranging in size from 0.5 to 3 microns (clay-size range) (Fig. 6D). The source of silica is probably the transformation of opal–A volcanic glass shards to quartz. Clay minerals are predominantly kaolinite, with illite and illite/smectite mixed-layer clay.

Bedding Types and Sedimentary Features

Hydrodynamic sedimentary features are common in Eagle Ford–A strata. Most of these hydrodynamic features indicate moderate to strong currents, including unidirectional and lesser oscillatory flow, affecting bottom sediments. Note that oscillatory and combined-flow currents can be generated both above and below storm-wave base (e.g., Mulder et al., 2009; Basilici et al., 2012), and oscillatory and combined-flow-current-produced sedimentary, hydrodynamic features cannot alone support the conclusion of whether the sea-bottom environment was above or below storm-wave base.

In the following subsections, the most common bedding types and sedimentary features are discussed. To make the section coherent, features have been assigned generally-accepted descriptive terms, and objective descriptive criteria are presented to describe the features. A short summary is provided to discuss whether the features formed above or below storm-wave base or whether their origins are ambiguous.

Hydrodynamic Features

Hummocky Cross-Stratification-Like and Swaley Cross-Stratification-Like Bedding. Hummocky cross-stratification-like (HCS–like) and swaley cross-stratification-like (SCS–like) bedding occurs in Eagle Ford–A strata (Figs. 7 and 8A). These two bedding types are commonly associated with one another, and the grains are very-fine allochems of planktic biota. HCS–like strata have a convex upper surface and a wavelength between crests of 1 and 5 ft (0.3 and 1.5 m) (Fig. 7). Relief of crests is less than 0.5 ft (15 cm), and these features are 0.5 to 1 ft (15 to 30 cm) thick (Fig. 7). Internal laminations are generally continuous packages of laminations pinching and swelling. SCS–like strata have a pinch-and-swell pattern, with many internal truncation surfaces (Fig. 7C).

These two types of stratification have been attributed to oscillatory flow associated with storm waves (e.g., Harms et al., 1975; Dott and Bourgeois, 1982; Hunter and Clifton, 1982), therefore leading Treviño (1988), Miller (1990), Donovan and Staerker (2010), and Minisini et al. (2018) to apply a storm or tempestite origin to the HCS–like and SCS–like strata in Eagle Ford–A section. Treviño (1988), Miller (1990), Donovan and Staerker (2010), and Minisini et al. (2018) proposed a storm-dominated shelf setting for the Eagle Ford–A without evaluating evidence provided by the biota or other sedimentary features. Lock and Fife (2004) and Lock et al. (2006, 2010b) suggested that these features are actually distorted turbidites, contourite ripples, and sand waves. They suggested that differential cementation (concretionary-like cementation) of grain-rich sediments interbedded with softer muds can produce sedimentary structures that at first glance appear to be hummocky cross-stratification.

It is suggested that HCS–like and SCS–like strata formed in an environment below storm-wave base, as suggested by Prave and Duke (1990) and Mulder et al. (2009, 2011). These workers recognized HCS–like and SCS–like strata in deepwater settings (1000 ft plus [300 m plus]) of the Upper Cretaceous in the Basque Pyrenees. Regional paleogeographic setting, associated deeper-water biota, and associated deeper-water features, such as

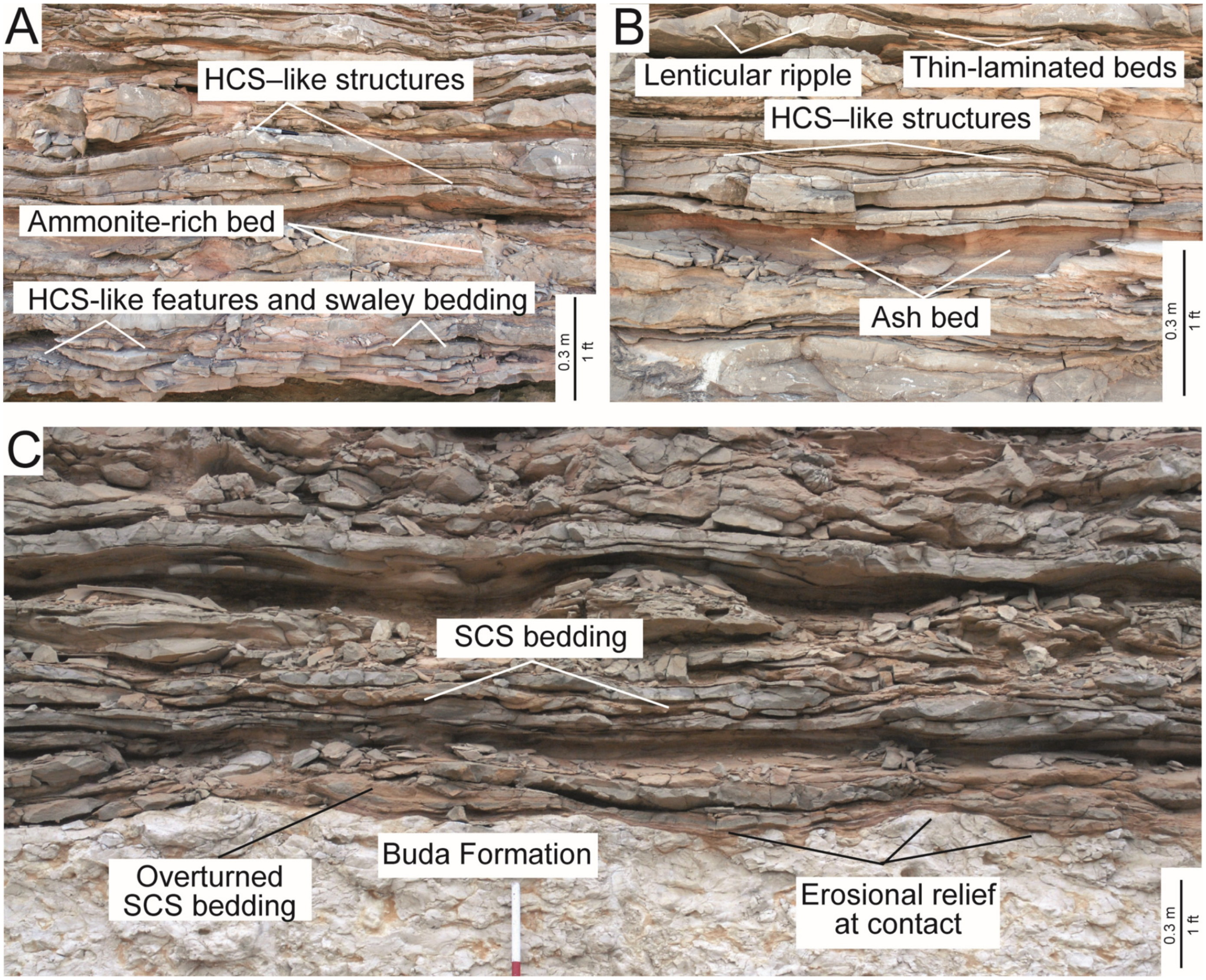

Figure 7. Hummocky cross-stratification (HCS–like) and swaley cross-stratification (SCS–like) bedding. (A) HCS–like and SCS–like bedding containing unit of ammonite-bearing packstone. (B) HCS–like and SCS–like cross-bedding. Also showing volcanic ash bed. (C) Interval of swaley cross-stratification.

debris flows, slumps, and slides, convinced them that these hydrodynamic structures were not produced above storm-wave base. The HCS–like and SCS–like strata they described are composed of fine- to medium-grained carbonate silt and are upwardly accreting hummocks with low-relief swales commonly occurring together—similar to the HCS–like and SCS–like strata in Eagle Ford–A strata. Within the turbidite sequence, Mulder et al. (2009, 2011) noted that HCS–like structures occur predominantly in the Bouma Tc interval and this is similar to what are seen in Eagle Ford–A section. They concluded that HCS–like and SCS–like strata are not related to oscillatory currents associated with storm waves but were generated in deeper water by standing waves forming at the upper-flow interface of turbidity currents (Mulder et al., 2009, 2011). Allen and Underhill (1989) also cautioned against applying oscillatory flow to HCS–like and SCS–like strata because they interpreted similar features in the Upper Jurassic Bencliff Grit in the U.K. as being deposited by unidirectional flow.

Frey (1990) studied burrowing of hummocky cross-stratification in Upper Cretaceous strata in the Western Cretaceous Seaway following storms. He found that post-storm burrowing was common and the sediment became highly bioturbated. Where storm waves produce hummocky cross-stratification, therefore, burrowing commonly followed as the bottom waters were oxygenated. No bioturbation followed the HCS–like features in Eagle Ford–A strata because the water column was stratified and sea bottom was below storm-wave base.

Turbidites. Some beds in Eagle Ford–A strata appear to be partial turbidite packages (Figs. 8A and 8B). Beds are plane (Bouma Tb units) to ripple bedded (Bouma Tc units), and these units are easily confused with rippled to mega-rippled bedding discussed in the next subsection (see Ripples and Megaripples). According to Stanley (1993), this confusion is common because following deposition of a turbidite, bottom currents can erode the turbidite, transforming it into a bottom-current structure. As noted in the previous section (see Hummocky Cross-Stratification-Like and Swaley Cross-Stratification-Like Bedding), the Bouma Tc unit can form HCS–like bedding (Fig. 8A).

Ripples and Megaripples. Ripples ranging in height from 0.1 to 0.5 ft (3 to 15 cm) are common (Figs. 8C and 8D) and

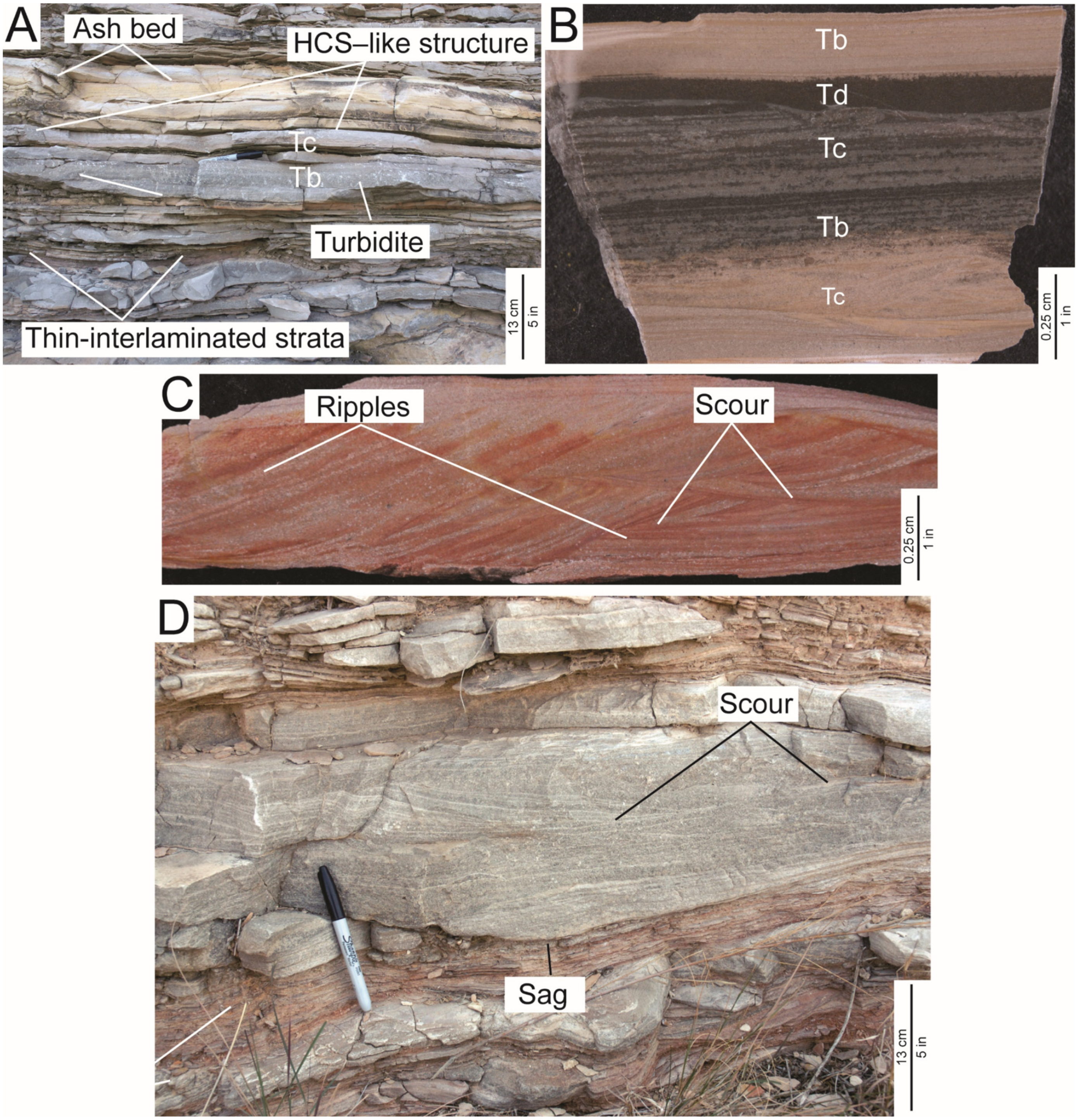

Figure 8. Examples of turbidites and ripples. (A) Turbidite unit showing Tb and Tc units, with Tc unit being HCS–like. (B) Rock slab with Bouma sequence bedding. (C) Unidirectional ripple stratification with scour surfaces. (D) Unidirectional megaripple that sagged into softer sediment below.

generally unidirectional, and they show internal crosscutting. Because most observations of ripples are only in two dimensions, some ripples that might be described as bidirectional may be related to absence of a three-dimensional view. Apparent bidirectional ripples are rare, if even present. Bottoms of some ripples display convex-down lamina that is related to settling into soft mud (Fig. 8C).

The ripples and megaripples in the Eagle Ford–A are interpreted as being related to bottom currents. Gravity-flow deposits are commonly reworked by bottom currents in deeper-water environments, and the product is ripples (e.g., Stanley, 1993). Stow et al. (1998) reported the occurrence of modern bottom-current sedimentary structures in water depths of 150 to 900 ft (45 to 275 m) (outer shelf/upper slope), which are within water depths postulated for Eagle Ford–A strata. They found that bottom-current sedimentary structures form in both siliciclastics and carbonates at these deeper-water depths under the influence of countercurrents, underflows, and major surface currents. Stanley (1993) described how turbidites are reworked into new sedimentary structures by bottom currents (see his figure 2 in Stanley [1993]). Initially the upper part of the turbidite is eroded and transformed into rippled units, and, as reworking continues, the turbidite continues to be eroded downward, producing beds of foreset laminae. With further downward erosion of the turbidite, lateral disruption of the bottom-current-reworked layer occurs, leaving behind lenticular lenses of foreset-laminated sediment (Figs. 7C, 7D, and 8). Similar sedimentary structures are common in Eagle Ford–A strata (Figs. 8C and 8D). Mutti (1992), in his atlas on turbidite sandstones, presented some excellent photographs of small-scale cross-stratification attributed to bottom-current reworking. These features are comparable to some cross-stratified beds in the Eagle Ford–A interval (see Mutti [1992, p. 274–275]).

Concentrated Flows. Several relatively massive units in the Eagle Ford–A section contain large, soft-sediment clasts and fewer lithoclasts (Fig. 9). These units are mud rich (kaolinite

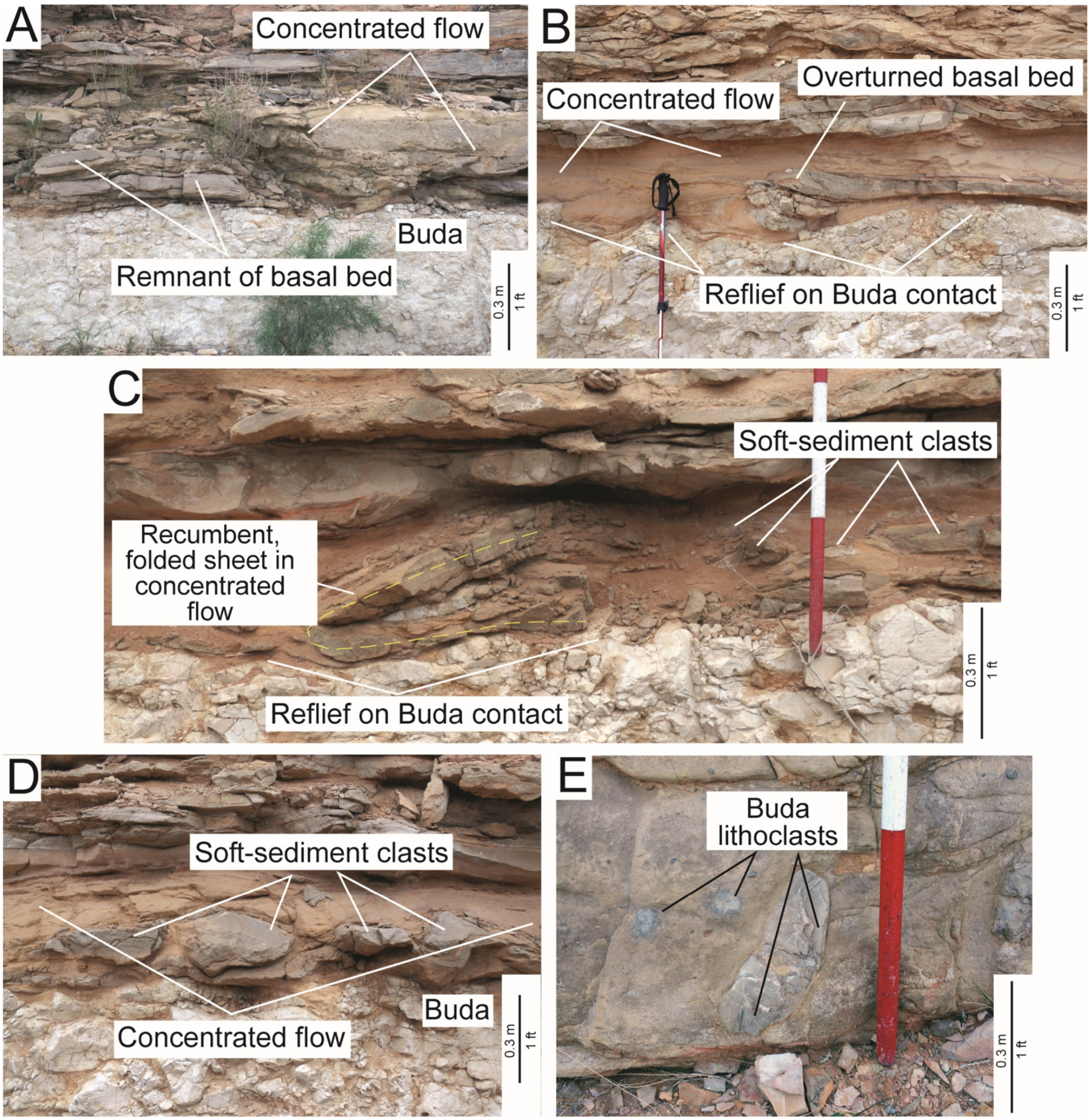

Figure 9. Concentrated flows. (A) Concentrated flow near base of Eagle Ford–A unit showing eroded remnant of basal unit. (B) Basal concentrated flow having scoured much of basal swaley bed. Slab of basal swaley bed preserved with edge of bed lifted up and overturned. (C) Basal, concentrated flow incorporating overturned sheet of swaley bedding. (D) Basal concentrated flow with soft-sediment clast of basal swaley unit. (E) Basal concentrated flow with Buda rounded lithoclasts.

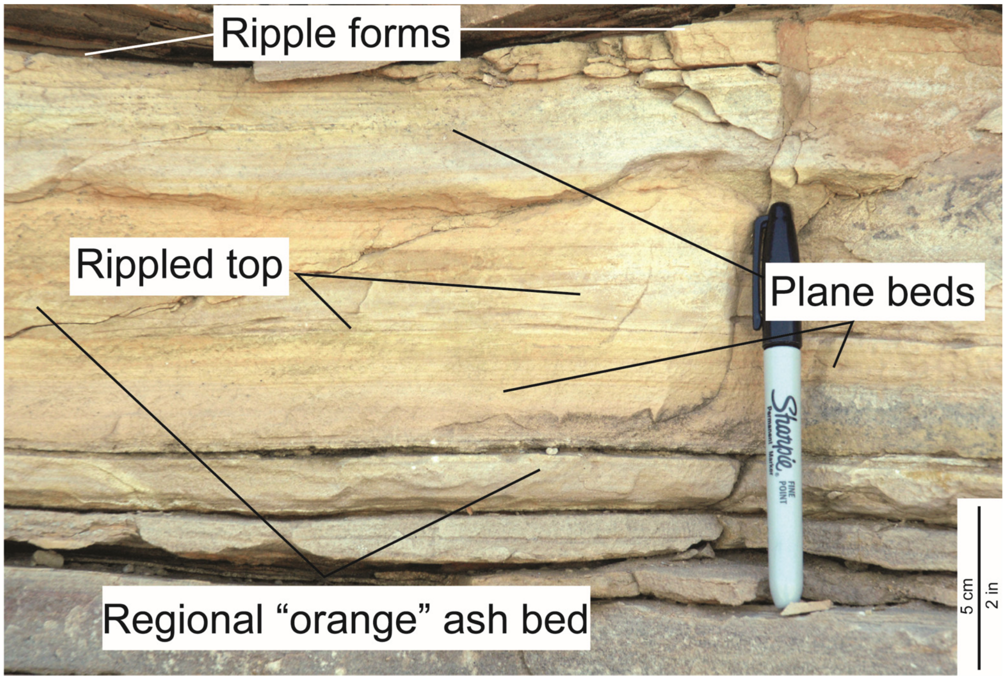

Figure 10. Regional "orange" volcanic ash bed. Internal sedimentary features suggesting ash bed reworked by turbidity or bottom currents.

clay that may be altered volcanic ash) and are interpreted as concentrated flow deposits. One distinctive layer, up to 3 ft (0.9 m) thick and near the base of the Eagle Ford–A section (Fig. 9), extends for tens of miles. The base of the flow was highly erosive, as indicated by the large-scale disruption and destruction of the swaley strata beneath the flow (Fig. 9). The lower swaley strata that was deposited in contact with the Buda section, are locally missing at the base of Eagle Ford–A (Fig. 9A), and parts of the swaley strata are overturned and folded (Figs. 9B and 9C). Soft-sediment clasts of the swaley strata, many showing contorted laminations, have been incorporated into the flow (Fig. 9D). Also, lithoclasts of Buda lithology have been incorporated (Fig. 9E). This flow unit is recognized in roadcuts over a broad area (>40 mi [>64 km] along strike [parallel to the shelf margin] and >15 mi [>24 km] along dip [perpendicular to the shelf margin]).

Interpreted concentrated flows in the Eagle Ford–A unit have many similarities as those described by Mulder and Alexander (2001). They found that concentrated flows can be strongly erosive, which supplies sediment to the flow. As noted earlier, the currents associated with the flow at the base of the Eagle Ford–A were strongly erosive. Mulder and Alexander (2001) also noted that concentrated flows can have long run-out distances, which is certainly the case for flows in Eagle Ford–A strata. Larger clasts can be entrained in concentrated flows, and this entrainment is seen in Eagle Ford–A strata as well. The clasts were likely supported by dispersive pressure and buoyancy (Mulder and Alexander, 2001).

Volcanic Ash Beds. Altered ash beds are common in the Eagle Ford–A section (Figs. 4, 6C, 6D, 10, 11A, and 12A), ranging in thickness from less than an inch to as much as 1 ft (0.3 m). Some beds show ripples and low-angle cross-stratification, indicating that some ash flows were reworked by bottom currents or emplaced by turbidity currents (Fig. 10). Lock et al. (2010b) displayed a slabbed sample with water-escape dish structures, which are indicative of rapid loading of sediment over previously-deposited soupy sediment.

Pierce et al. (2016) concluded that the source of the volcanic ashes in Eagle Ford–A strata is volcanism in northern Mexico and southern Arizona. Evenness and continuity of ash beds suggest deposition by ash falling on the ocean surface and settling onto the seafloor by suspension. Preservation as distinct units over broad areas (tens of miles) indicates that they were not reworked by storm waves impinging on the sea bottom or by bioturbation—further evidence that deposition of Eagle Ford–A strata was below storm-wave base in an anoxic setting. Some localized, short sections of the ash beds were scoured out by bottom currents.

Channels. Dip-directed channels (south) are common (Figs. 4A, 4B, and 11). They range in depth from 1 to 5 ft (0.3 to 1.5) and in width from a few feet to nearly 40 ft (13 m). The channels cut out enclosing strata, and the fill is chaotic, with much of the material appearing to be contorted, transported bundles of soft sediments. Lock and Peschier (2006) also noted shallow channels or scours in the Eagle Ford–A strata.

Soft-Sediment-Deformation Features

Slumps or Surge-Like Flows. Several thick units (3 to 6 ft thick [0.9 to 1.8 m]) in the Eagle Ford–A section are widespread (tens of miles) slumps or surge-like flows (mass transport deposits) (Figs. 4, 11, and 12). Original bedding is highly deformed and transported. Contemporaneous deformation structures include recumbent folds (Fig. 12A), small to large transported blocks (e.g., Fig. 12), and disturbed and folded bedding (rafted sheets) (Fig. 12). Some of the units appears to have carved channels (e.g., Fig. 4A) that are filled with chaotic material, as noted in the section on Channels. Lock and Peschier (2006) noted that these features occurred over a geographic area from Big Bend to Del Rio.

Soft-sediment deformation features such as these can be common on platforms with low-angle slopes (e.g., Enos and Moore, 1983; Hance, 2003). Differential liquefaction and fluidization triggered by storm-wave loading can also produce soft-sediment deformation features on a shelf (Chen and Lee, 2013). Storm-triggered loading is discounted for these deposits because the carbonate breccia bodies areal distribution produced by this mechanism do not match the breccia bodies in Eagle Ford–A strata. Also, channel-like features noted in the Eagle Ford–A were not recognized in the carbonate storm bodies of Chen and Lee (2013). In the study by Chen and Lee (2013), carbonate

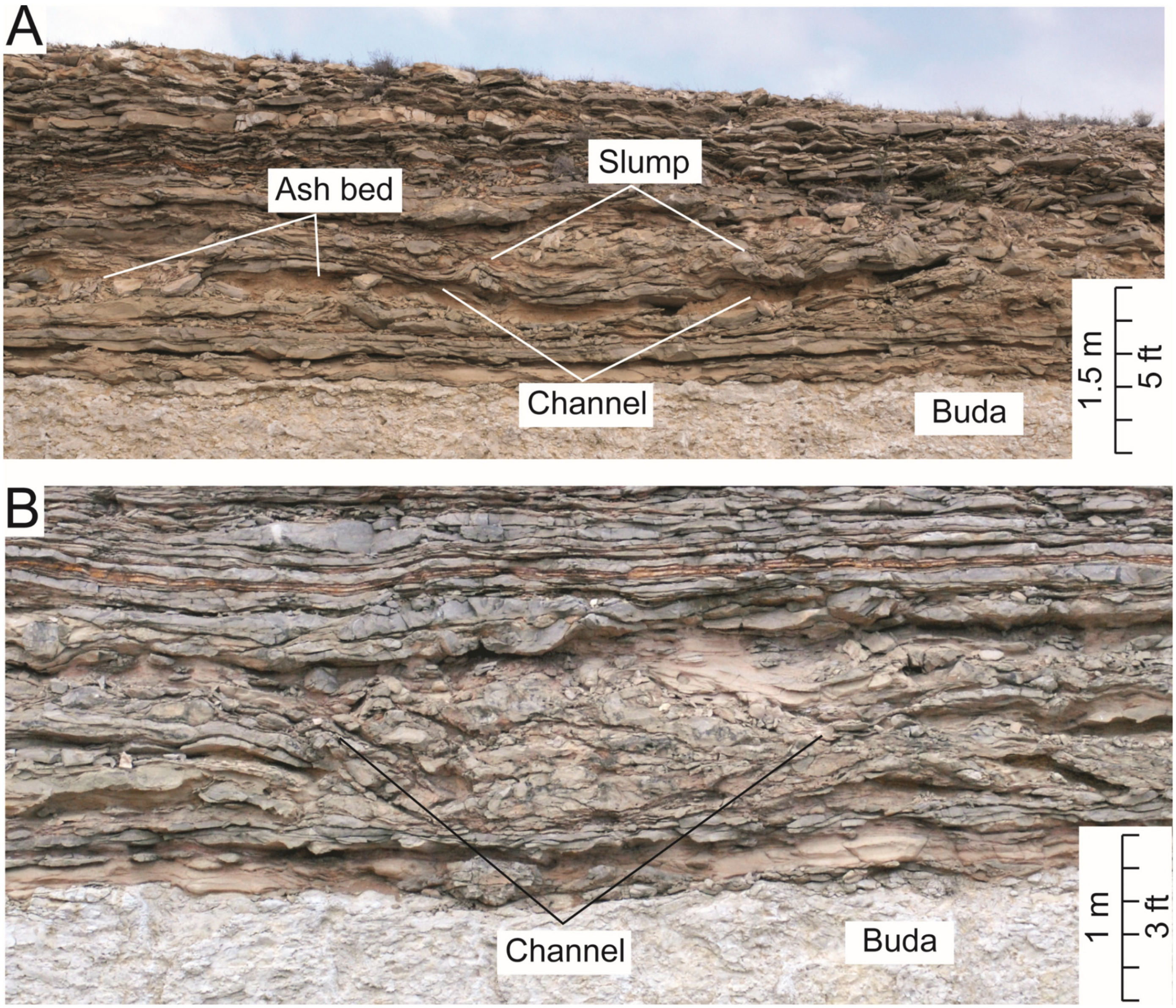

Figure 11. Channel features. (A) Channel in Eagle Ford–A unit showing fill of contorted strata. (B) Small channel showing scour of adjacent strata and fill of chaotic material.

sediment appears to be dominantly oolitic, reflecting a high-energy shallow shelf, whereas Eagle Ford–A strata are composed of open-marine, low-energy pelagic sediments.

Highly-disturbed units in the Eagle Ford–A unit cover a wide area greater than 40 mi (64 km) along strike and at least 15 mi (24 km) in the dip direction. A regional triggering mechanism such as earthquakes is necessary. Earthquakes are well recognized as a triggering mechanism for soft-sedimentation deformation (e.g., Owen et al., 2011; Moretti and van Loon, 2014). As noted by Pierce et al. (2016), volcanism was active both in northern Mexico and southern Arizona, and this volcanism could have triggered large earthquakes regionally.

Slides. Slide deformation is present near the top of the Eagle Ford–A section (Fig. 4C), expressing shear in the form of normal and overturned folds, as well as thrusted sheets of sediment. Slides indicate downslope movement of the sediment mass, suggesting a slight slope to the platform. The unit (Fig. 4C) affected is approximately 4 ft (1.2 m) thick.

Load Structures. The base of some units displays load features similar to ball-and-pillow structures. These are products of rapid loading of sediments on fluid-rich, muddier sediments below (Weaver and Jeffcoat, 2009).

EAGLE FORD–A INTRASTRATAL ARCHITECTURE

Eagle Ford–A strata can be divided into seven general correlative subunits (Fig. 4) that are partly depositional and partly related to regional, soft-sediment-deformation events. Figure 4 shows the stacking of subunits seen in most roadcuts. Although the lower soft-sediment-deformation event (subunit 4) is seen in all roadcuts investigated, the upper soft-sediment-deformation event (subunit 6) is not.

Subunit 1 (Fig. 4), which immediately overlies the Buda Formation, is swaley and ranges in thickness from 0.6 to 1 ft (1.8 to 0.3 m). Small-scale solution troughs or potholes are developed on the Buda unconformable surface (Fig. 13) and these surface depressions are filled with wavy Eagle Ford globigerinid packstone. Subunit 1 was extensively eroded (Fig. 9) by concentration-flow currents that deposited subunit 2. In many areas,

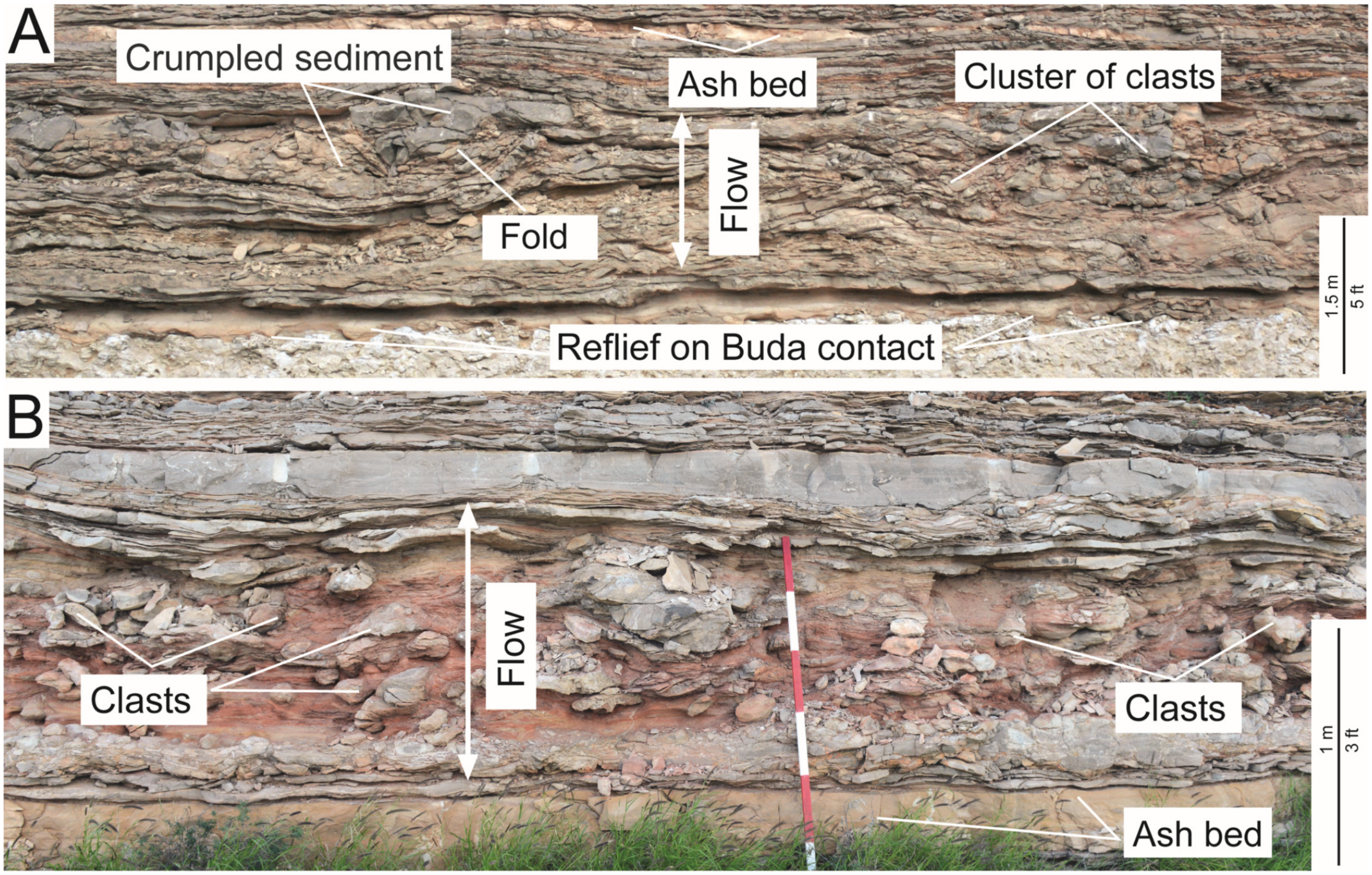

Figure 12. Slump to surge-flow deposits. (A) Mass-movement strata showing highly-disturbed bedding and some scour of adjacent strata. (B) Slump appearing more like debris flow, with numerous clasts within fine-grained matrix.

subunit 1 is partially to totally missing (Fig. 13), and some of the subunit 1 beds are curled up and overturned on themselves (Figs. 9A–9C). Soft-sediment clasts (some tabular) of subunit 1, ranging to several feet thick, are incorporated into subunit 2 (Fig. 4). These soft-sediment clasts show highly-disturbed and contorted bedding with no brittle fractures, indicating that the sediment was ductile at the time of erosion.

Subunit 2 is characterized by abundant soft-sediment clasts and rare lithoclasts (Figs. 9C and 9D) and is interpreted as a volcanic-ash- and carbonate-sediment-rich concentrated flow (Fig. 9) ranging from 1 to 3 ft thick (0.3 to 0.9 m). Soft-sediment clasts are ripped-up pieces of subunit 1 and the lithoclasts are rounded, ripped-up Buda rock fragments. Channeling is noted, as well as low-angle bedding that may be lateral accretionary units. This subunit can be seen in roadcuts north of Del Rio along Highway 377 to farther west near Langtry along Highway 90.

Unit 3, which is approximately 4 to 5 ft thick (1.2 to 1.5 m), displays no soft-sediment deformation and is composed of swaley and hummock-like bedding similar to subunit 1. Saccocomid fragments are common.

Subunit 4 (Fig. 4) is defined by extensive soft-sediment deformation. The original bedding of the strata was probably the same as that of the strata in subunits 1 and 3. The subunit is characterized by extensive slumps, slides, masses of contorted and convoluted soft-sediment, and soft-sediment clasts of various sizes. Within this highly-disturbed subunit, some channeling (e.g., Fig. 11A) is present that cuts out individual beds. It ranges in thickness from 2 to 4 ft (0.6 to 1.2 m).

Subunit 5 (Fig. 4) is similar to subunits 1 and 3, being composed of swaley and hummock-like bedding. It is 3 ft (1 m) thick.

Subunit 6 (Fig. 4), where developed, is similar to subunit 4. It is a widespread, disrupted subunit, 2 to 3 ft thick (0.6 to 0.9 m), with abundant slumps, slides, masses of contorted and convoluted soft-sediment slabs, and soft-sediment clasts of various sizes. It is not as continuous as the disrupted layer in subunit 4.

Subunit 7 (Fig. 4) is similar to subunits 1, 3, and 5 and ranges in thickness from 2 to 3 ft (0.6 to 0.9 m). The upward contact, gradational with the Eagle Ford–B strata above (Fig. 4C), is placed just below where the globigerinid-rich beds become planar bedded and laterally continuous (Figs. 4A and 4C).

DISCUSSION

As Basilici et al. (2012) noted, many authors (e.g., Lamb et al., 2008; Mulder et al., 2009) have addressed the problem of interpreting sedimentary features to delineate deposition above or below storm-wave base. In cases of siliciclastic sedimentation, grain types add little to identifying depositional position relative to storm-wave base, whereas with carbonate sedimentation grain types provide significant information about depositional setting. In this discussion, an integration of regional depositional setting, assemblage of biota, sedimentary features, and soft-sediment-deformational structures is analyzed to define the most logical depositional setting for Eagle Ford–A strata. This interpretation of depositional setting must balance evidence gleaned from biotas, interpreted sedimentary features, and soft-sediment-deformational structures.

As discussed earlier, Eagle Ford–A strata were deposited on a drowned carbonate platform approximately 75 mi (120 km) from the paleoshelf edge, which was a raised rimmed margin relative to the platform interior (Alnahwi et al., in press). Lock and Fife (2004) and Lock et al. (2010b) also concluded that the

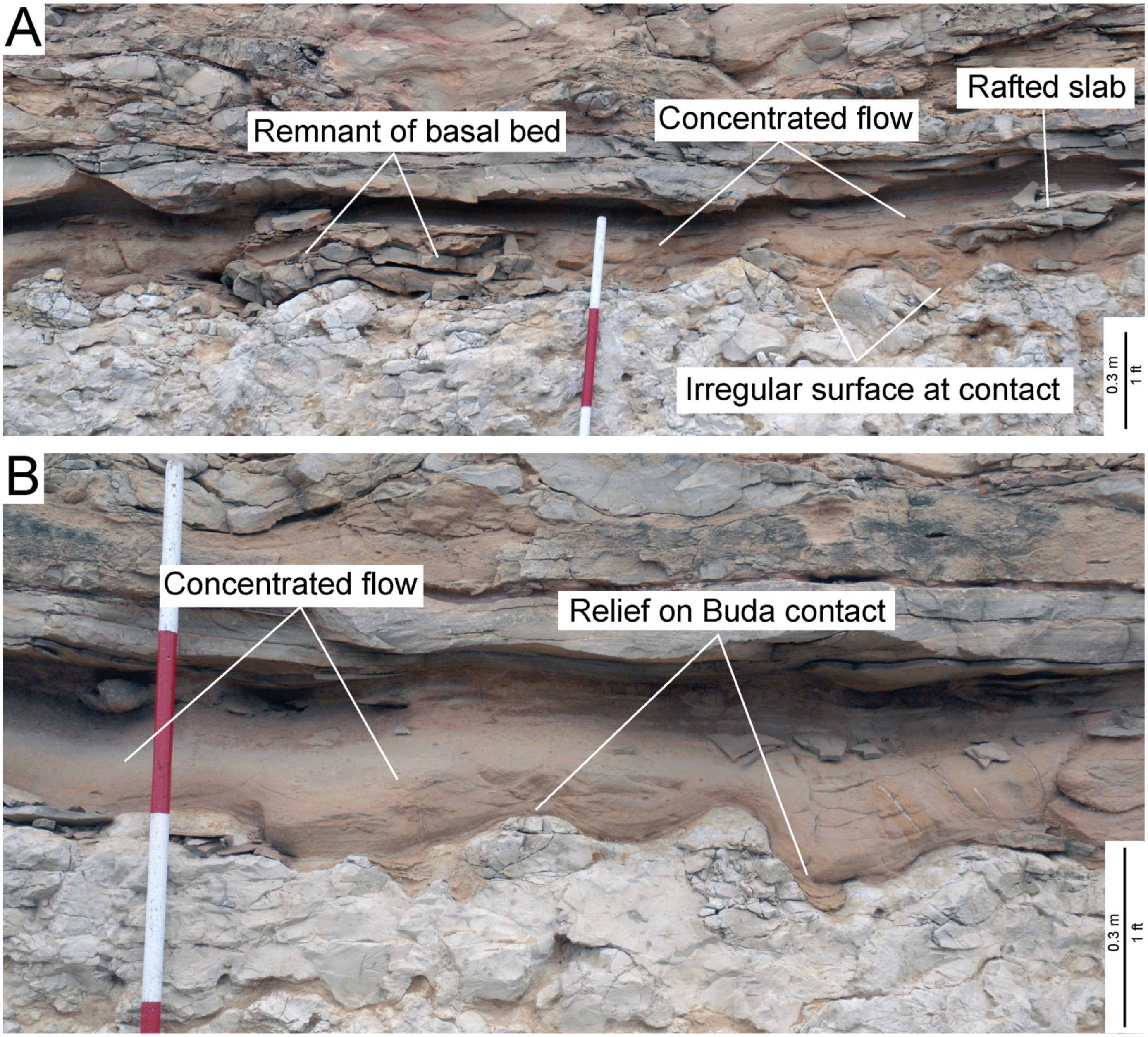

Figure 13. Contact surface between Buda Formation and Eagle Ford–A section. (A) Buda surface with irregular surface appearing to have been lithified by time of Eagle Ford–A deposition. Patch of remnant, basal, swaley Eagle Ford–A preserved on Buda surface. (B) Differential relief along surface of Buda Formation. No alteration of Buda surface noted.

setting in this study area was in deeper water (greater than 300 ft [100 m]). During deposition of Eagle Ford–A strata, the raised rim may have aided in restriction of the basin. Circulation on a restricted Eagle Ford–A shelf would have been less efficient than if the shelf had been completely open to deeper water of the paleo–Gulf of Mexico. The Eagle Ford–A drowned shelf was generally flat, except around margins of interior basins, such as the Maverick Basin to the south. In the area of investigation, the platform was considered to be relatively flat, with a gentle dip estimated to be less than 1°. Note that mass movements, as seen in Eagle Ford–A strata, can occur on slopes of ±0.5° and that most areally-extensive mass flows are associated with lower slopes (Hance, 2003).

The biota is composed predominantly of coccolith and coccolith elements, globigerinids, coccolithophores, and saccocomid fragments, which are all planktic organisms that favored distal, deeper- and quieter-water, open-marine settings (Flügel, 2004, p. 91). This population of organisms did not thrive in nearshore, higher-energy, agitated, and turbulent waters. Total lack of bioturbation, absence of benthic biotas except transported inoceramid fragments, and raised levels of TOC strongly support dysaerobic to anaerobic bottom waters and sediments. Treviño (1988) and Lock and Peschier (2006) came to the same conclusion about anoxic bottom conditions during Eagle Ford–A deposition. To account for this dissimilarity abundance of organisms living in the shallower-surface water column relative to the deeper bottom water column, a stratified water column with a pycnocline must be invoked.

Sedimentary features and associated flow processes in the Eagle Ford–A show characteristics of both unidirectional and lesser oscillatory currents. A major question is whether sedimentary features produced by oscillatory-like currents support deposition only above storm-wave base or whether oscillatory-like currents occur and affect sediments below storm-wave base. Mutti et al. (2003) and Basilici et al. (2012) are among several studies noting that the oscillatory component of combined flow can have various origins, including internal waves, reflected turbidity currents, and superficial waves. Allen and Underhill (1989, p. 241) stated that because "undulatory forms of stratification are substrate- and process-dependent and not environmentally specific, great care must be taken in the interpretation of paleoenvironmental settings." Position of Eagle Ford–A strata on a drowned platform associated with open-marine, planktic biota is important evidence towards whether deposition occurred above or below storm-wave base. A deeper-water setting would not favor storm-wave-produced features but would favor features produced by hyperpycnal gravity flows resedimenting updip deepwater-derived planktic sediments.

Eagle Ford–A strata are rich in sedimentary features, some of which are debatable as to whether they were deposited by oscillatory or combined flow currents. According to many studies, such as Harms et al. (1975), Dott and Bourgeois (1982), Hunter and Clifton (1982), Leckie and Walker (1982), and Dumas and Arnott (2006), swaley and hummocky cross-stratification occur above storm-wave base, and, according to Dumas and Arnott (2006), swaley bedding forms shallower in the water column than hummocky bedding. Their stance is based on the presence of sedimentary features that they thought had been formed by oscillatory or combined flow currents. However, other authors, such as Prave and Duke (1990) and Mulder et al. (2009), documented HCS–like crossbedding in the deepwater setting of the Basque Flysch series in France. Mulder et al. (2009) provided a concise discussion of HCS–like features and how oscillatory currents could construct these features above and below storm-wave base. Allen and Underhill (1989) proposed situations in which swaley cross-stratification forms under highly sediment-charged, unidirectional flow. Most of the debatable investigations that settled on an above-storm-wave base setting are in siliciclastic deposits. The study by Mulder et al. (2009) is in deepwater carbonates, which are composed of deepwater, planktic biota. The dominance of planktic biota in a basinal setting provided evidence for deeper-water sedimentation. Therefore, as documented in Eagle Ford–A strata, a deeper-water planktic biota without benthic organisms is evidence of deposition on a deep, drowned shelf below storm-wave base. The sedimentary features recorded were deposited by hyperpycnal flows consisting of concentrated flows and low-density turbidites. Some of these flows were modified by deeper-water bottom currents similar to those documented in Eagle Ford–B strata (Frébourg et al., 2016).

The interpretation of the depositional setting of Eagle Ford–A strata is based on biota, sedimentary features, and TOC. We understand that some HCS–like and SCS–like bedding can be considered to be related to above-storm-wave base processes, given the concept that these features must form from oscillatory or combined flow and these flow types are related directly to gravity-wave-generated currents. However, the Eagle Ford–A biota does not support an above-storm-wave-base origin. It dictates a deeper-water environment where bottom waters were dysaerobic or anaerobic. This biota did not thrive in a nearshore, wave-dominated setting; the organisms preferred a quiet-water, lower-energy, open-marine setting. Therefore, the interpretation of an open-marine, below-storm-wave base setting with anaerobic bottom waters honors both the biological and physical evidence documented in Eagle Ford–A strata.

CONCLUSIONS

The depositional setting that produced sedimentary features in Eagle Ford–A strata in the study area may be debatable, but evidence provided by the biota, including lack of bioturbation and elevated TOC, is not debatable. Sedimentary features must be viewed within the context of these additional parameters.

Eagle Ford–A strata in southwestern Texas were deposited on a drowned shelf, below storm-wave base, in a dysaerobic or anaerobic environment. The biota supports deeper-water bottom conditions, lack of burrowing and raised TOC supporting dysaerobic or anaerobic bottom conditions, sedimentary features supporting hyperpycnal gravity flows that were reworked by bottom currents, and slumps and slides supporting a low-angle, inclined drowned shelf.

This study, along with other studies (e.g., Mulder et al., 2009; Basilici et al., 2012), again emphasizes that sedimentary features alone may not be enough evidence to define a depositional setting definitively. Also, no one sedimentary feature, such as HCS–like or SCS–like bedding, can override other significant evidence. *All* evidence must be considered and balanced to provide the most logical interpretation.

ACKNOWLEDGMENTS

We want to thank the Mudrock System Research Laboratory (MSRL) and the Carbonate Reservoir Characterization Research Laboratory (RCRL) at the Bureau of Economic Geology and associated sponsors for support of this investigation. Discussions with Stephen Ruppel, William Galloway, Greg Frébourg, Alton Brown, Daniel Minisini, William Morris, and Art Donovan are especially appreciated. This manuscript was edited by Lana Dieterich, consultant to the Bureau of Economic Geology. Patrick Smith of the Bureau helped with the SEM images. Evan Sivil and David Smith helped the author complete initial fieldwork. Stephen Ruppel, Lowell Waite, Brian Lock, and James Willis reviewed the manuscript and provided valuable feedback and suggestions for improvement. Publication authorized by the Director, Bureau of Economic Geology, Jackson School of Geosciences, University of Texas at Austin.

REFERENCES CITED

Allen, P. A., and J. R. Underhill, 1989, Swaley cross-stratification produced by unidirectional flows, Bencliff Grit (Upper Jurassic), Dorset, UK: Journal of the Geological Society, v. 146, p. 241–252, doi:10.1144/gsjgs.146.2.0241.

Alnahwi, A., R. G. Loucks, S. C. Ruppel, R. W. Scott, and N. Tribovillard, in press, Dip-related changes in stratigraphic architecture and associated sedimentological and geochemical variability in the Upper Cretaceous Eagle Ford Group in South Texas: American Association of Petroleum Geologists Bulletin.

Balch, W. M., 2004, Re-evaluation of the physiological ecology of coccolithophores, *in* H. R. Thierstein and J. R. Young, eds., Coccolithophores—From molecular processes to global impact: Springer-Verlag, Berlin, Heidelberg, Germany, p. 165–190, doi:10.1007/978-3-662-06278-4_7.

Basilici, G., P. H. Vieire de Luuca, and D. G. Poire, 2012, Hummocky cross-stratification-like structures and combined-flow ripples in the Punta Negra Formation (Lower-Middle Devonian, Argentine Precordillera): A turbiditic deep-water or storm-dominated prodelta inner-shelf system?: Sedimentary Geology, v. 267–268, p. 73–92, doi:10.1016/j.sedgeo.2012.05.012.

Bé, A. W. H., 1960, Ecology of recent planktonic foraminifera: Part 2: Bathymetric and seasonal distributions in the Sargasso Sea off Bermuda: Micropaleontology, v. 6, p. 373–392, doi:10.2307/1484218.

Blakey, R. C., 2018, Paleogeography and geologic evolution of North America: Images that track the ancient landscapes of North America (Late Cretaceous–100 Ma): Northern Arizona University School of Earth Sciences and Environmental Sustainability, Flagstaff, <http://jan.ucc.nau.edu/rcb7/nam.html> Last accessed April 30, 2018.

Boltovskoy, E., and R. Wright, 1976, Planktonic foraminifera: Springer, Dordrecht, Netherlands, 515 p., doi:10.1007/978-94-017-2860-7.

Boucot, A. J., 1990, Evolutionary paleobiology of behavior and coevolution: Elsevier Science Publishers, Amsterdam, The Netherlands, 724 p.

Broerse, A. T. C., P. Ziveri, J. E. van Hinte, and S. Honjo, 2000, Coccolithophore export production, species composition and coccolith–$CaCO_3$ fluxes in the NE Atlantic (34ºN 21ºW and 48ºN 21ºW): Deep-Sea Research II, v. 47, p. 1877–1906, doi:10.1016/s0967-0645(00)00010-2.

Bromley, R. G., 1990, Trace fossils: Biology, taphonomy and applications: Unwin Hyman, London, U.K., 280 p.

Casey, R., J. M. Spaw, F. Kunze, E. Reynolds, T. Duis, K. McMillen, D. Pratt, and V. Anderson, 1979, Radiolarian ecology and the development of the radiolarian component in Holocene sediments, Gulf of Mexico and adjacent seas with potential paleontological applications: Gulf Coast Association of Geological Societies Transactions, v. 29, p. 228–237.

Chen, J., and H. S. Lee, 2013, Soft-sediment deformation structures in Cambrian siliciclastic and carbonate storm deposits (Shandong Province, China): Differential liquefaction and fluidization triggered by storm-wave loading: Sedimentary Geology, v. 288, p. 81–94, doi:10.1016/j.sedgeo.2013.02.001.

Denne, R. A., R. E. Hinote, J. A. Breyer, T. H. Kosanke, J. A. Lees, N. Engelhardt-Moore, J. M. Spaw, and N. Tur, 2014, The Cenomanian-Turonian Eagle Ford Group of South Texas: Insights on timing and paleoceanographic conditions from geochemistry and micropaleontologic analyses: Palaeogeography, Palaeoclimatology, Palaeoecology, v. 413, p. 2–28, doi:10.1016/j.palaeo.2014.05.029.

Donovan, A. D., and T. S. Staerker, 2010, Sequence stratigraphy of the Eagle Ford (Boquillas) Formation in the subsurface of South Texas and the outcrops of West Texas: Gulf Coast Association of Geologic Societies Transactions, v. 60, p. 861–899.

Donovan, A. D., T. S. Staerker, A. Pramudito, W. Li, M. J. Corbett, C. M. Lowery, A. M. Romero, and R. D. Gardner, 2012, The Eagle Ford outcrops of West Texas: A field laboratory for understanding heterogeneities within unconventional mudstone reservoirs: Gulf Coast Association of Geological Societies Journal, v. 1, p. 162–185, <http://gcags.org/Journal/2012.GCAGS.Journal/GCAGS.Journal.2012.vol1.p162-185.Donovan.et.al.pdf> Last accessed August 2, 2018.

Donovan, A. D., R. D. Gardner, A. Pramudito, T. S. Staerker, M. Wehner, M. J. Corbett, J. J. Lundquist, A. M. Romero, L. C. Henry, J. R. Rotzien, and K. S. Boling, 2015, Chronostratigraphic relationships of the Woodbine and Eagle Ford groups across Texas: Gulf Coast Association of Geological Societies Journal, v. 4, p. 67–87, <http://gcags.org/Journal/2015.GCAGS.Journal/2015.Journal.v4.5.p67-87.Donovan.et.al.press.pdf> Last accessed August 2, 2018.

Dott, R. H., and J. Bourgeois, 1982, Hummocky stratification: Significance of its variable bedding sequences: Geological Society of America Bulletin, v. 93, p. 663–680, doi:10.1130/0016-7606(1982)93<663:HSSOIV>2.0.CO;2.

Dumas, S., and R. W. C. Arnott, 2006, Origin of hummocky and swaley cross-stratification—The controlling influence of unidirectional current strength and aggradation rate: Geological Society of America Bulletin, v. 34, p. 1073–1076, doi:10.1130/G22930A.1.

Earth Observatory, 2018, EOS Project Science Office, NASA Goddard Space Flight Center, <https://earthobservatory.nasa.gov/Features/Coccolithophores/coccolith_2.php> Last accessed April 24, 2018.

Ekdale, A. A., and T. R. Mason, 1988, Characteristic trace fossil associations in oxygen-poor sedimentary environments: Geology, v. 16, p. 720–723, doi:10.1130/0091-7613(1988)016<0720:CTFAIO>2.3.CO;2.

Eldrett, J. S., C. Ma, S. C. Bergman, B. Lutz, F. J. Gregory, P. Dodsworth, M. Phipps, P. Hardas, D. Minisini, A. Ozkan, J. Ramezani, S. A. Bowring, S. L. Kamo, K. Ferguson, C. Macaulay, and A. E. Kelly, 2015, An astronomically calibrated stratigraphy of the Cenomanian, Turonian and earliest Coniacian from the Cretaceous Western Interior Seaway, USA: Implications for global chronostratigraphy: Cretaceous Research, v. 56, p. 316–344, doi:10.1016/j.cretres.2015.04.010.

Enos, P., and C. H. Moore, 1983, Fore-reef slope, *in* P. A. Scholle, D. G. Bebout, and C. H. Moore, eds., Carbonate depositional environments: American Association of Petroleum Geologists Memoir 33, Tulsa, Oklahoma, p. 507–614, doi:10.1002/gj.3350190407.

Flügel, E., 2004, Microfacies of carbonate rock: Analysis, interpretation and application: Springer-Verlag, Berlin, Heidelberg, Germany, 976 p., doi:10.1007/978-3-662-08726-8.

Frébourg, G., S. Ruppel, R. Loucks, and J. Lambert, 2016, Depositional controls on sediment body architecture in the Eagle Ford/Boquillas system: Insights from outcrops in West Texas, United States: American Association of Petroleum Geologists Bulletin, v. 4, p. 657–682, doi:10.1306/12091515101.

Frey, R. W., 1990, Trace fossils and hummocky cross-stratification, Upper Cretaceous of Utah: *Palaios*, v. 5, p. 203–218, doi:10.2307/3514939.

Gradstein, F. M., J. G. Ogg, M. D. Schmitz, and G. Ogg, 2012, The geologic time scale 2012: Elsevier, Boston, Massachusetts, 1176 p.

Guerreiro, C. C. V., 2013, Paleoecology of coccolithophores in the submarine canyons of the central Portuguese continental margin: Environmental, sedimentary and oceanographic implications: Ph.D. Dissertation, University of Lisbon, Portugal, 252 p.

Hance, J. J., 2003, Submarine slope stability: Report prepared for the Minerals Management Service under the MMS/OTRC Cooperative Research Agreement 1435–01–99–CA–31003, Task Order 18207, MMS Project 421, 245 p., <https://www.bsee.gov/sites/bsee.gov/files/tap-technical-assessment-program//421ab.pdf> Last accessed August 18, 2018.

Harms, J. C., J. B. Southard, D. R. Spearing, and R. G. Walker, 1975, Depositional environments as interpreted from primary sedimentary structures and stratification sequences: Society of Economic Paleontologists and Mineralogists Short Course 2, Tulsa, Oklahoma, 161 p., doi:10.2110/scn.75.02.

Hazzard, R. T., 1959, Diagrammatic-stratigraphic sections Lozier Canyon section, Terrell County, Texas, *in* R. L. Cannon, R. T. Hazzard, A. Young, and K. P. Young (leaders), Geology of the Val Verde Basin and field trip guidebook: West Texas Geological Society, Midland, Texas, 118 p.

He, Y., J. Luo, X. Li, Z. Gao, and Z. Wen, 2011, Evidence of internal-wave and internal-tide deposits in the Middle Ordovician Xujiajuan Formation of the Xiangshan Group, Ningxia, China: Geo-Marine Letters, v. 31, p. 509–523.

Hunter, R. E., and H. Clifton, 1982, Cyclic deposits and hummocky cross-stratification of probable storm origin in Upper Cretaceous rocks of the Cape Sebastian area, southwestern Oregon: Journal of Sedimentary Research, v. 52, p. 127–143.

Lamb, M. P., P. M. Myrow, C. Likens, K. Houck, and J. Strauss, 2008, Deposits from wave-influenced turbidity currents: Pennsylvanian Minturn Formation, Colorado: Journal of Sedimentary Research, v. 78, p. 480–498, doi:10.2110/jsr.2008.052.

Landman, N. H., and J. R. Geyssant, 1993, Heterochrony and ecology in Jurassic and Cretaceous ammonites: Geobios, v. 26, p. 247–255, doi:10.1016/S0016-6995(06)80379-7.

Leavesley, A., M. Bauer, K. McMillen, and R. Casey, 1978, Living shelled microzooplankton (radiolarians, foraminiferans, and pteropods) as indicators of oceanographic processes in water over the outer continental shelf of South Texas: Gulf Coast Association of Geological Societies Transactions, v. 28, p. 229–238.

Leckie, D. A., and R. G. Walker, 1982, Storm- and tide-dominated shorelines in Cretaceous Moosebar–Lower Gates interval—Outcrop equivalents of deep basin gas trap in Western Canada: American Association of Petroleum Geologists Bulletin, v. 66, p. 138–157, doi:10.1306/03B59A53-16D1-11D7-8645000102C1865D.

Lock, B. W., and A. W. Fife, 2004, Contourites and related outer shelf/upper slope sediments, Boquillas Formation, West Texas: American Association of Petroleum Geologists Search and Discovery Article 90026, Tulsa, Oklahoma, 1 p., <http://www.searchanddiscovery.com/abstracts/html/2004/annual/abstracts/Lock.htm> Last accessed August 27, 2018.

Lock, B. E., and L. Peschier, 2006, Boquillas (Eagle Ford) upper slope sediments, West Texas: Outcrop analogs for potential shale reservoirs: Gulf Coast Association of Geological Societies Transactions, v. 56, p. 491–508.

Lock, B. E., F. S. Bases, and R. A. Glaser, 2007, The Cenomanian sequence stratigraphy of Central to West Texas: Gulf Coast Association of Geological Societies Transactions, v. 57, p. 465–479.

Lock, B. E., R. W. Butler, and R. T. Franklund, 2009, Tempestite sedimentation: An example from the Del Rio Formation of West Texas: Gulf Coast Association of Geological Societies Transactions, v. 59, p. 463–476.

Lock, B. E., L. Peschier, A. Fife, and B. Wawak, 2010a, Eagle Ford (Boquillas) Formation and associated strata in Val Verde County, Texas: South Texas Geological Society Guidebook 2010–01 in association with Gulf Coast Association of Geological Societies Annual Meeting, San Antonio, 82 p.

Lock, B. E., L. Peschier, and N. Whitcomb, 2010b, The Eagle Ford (Boquillas Formation) of Val Verde County, Texas—A window on the South Texas play: Gulf Coast Association of Geological Societies Transactions, v. 60, p. 419–434.

Lock, B. E., J. W. Grimball, and J. G. Johnson, 2013, The Cenomanian Del Rio Formation in West Texas: Gulf Coast Association of Geological Societies Transactions, v. 63, p. 331–342.

Lowery, C. M., M. J. Corbett, R. M. Leckie, D. Watkins, A. M. Romero, and A. Pramudito, 2014, Foraminiferal and nannofossil paleoecology and paleoceanography of the Cenomanian-Turonian Eagle Ford Shale of southern Texas: Palaeogeography, Palaeoclimatology, Palaeoecology, v. 413, p. 49–65, doi:10.1016/j.paleo.2014.07.025.

MicrobeWik, 2018, Radiolaria, <https://microbewiki.kenyon.edu/index.php/Radiolaria> Last accessed March 4, 2018.

Miller, R. W., 1990, The stratigraphy and depositional environment of the Boquillas Formation of southwest Texas: M.S. Thesis, University of Texas at Arlington, 156 p.

Minisini, D., J. Eldrett, S. C. Bergman, and R. Forkner, 2018, Chronostratigraphic framework and depositional environments in the organic-rich, mudstone-dominated Eagle Ford Group, Texas, USA: Sedimentology, v. 65, p. 1520–1557, doi:10.1111/sed.12437.

Moore, R. C., 1967, Unique stalked crinoids from Upper Cretaceous of Mississippi: University of Kansas Paleontological Contributions Paper 17, Lawrence, 36 p., <https://kuscholarworks.ku.edu/handle/1808/3676> Last accessed August 2, 2018.

Moretti, M., and A. J. van Loon, 2014, Restrictions to application of 'diagnostic' criteria for recognizing ancient seismites: Journal of Palaeogeography, v. 3, p. 162–173, doi:10.3724/SP.J.1261.2014.00050.

Mulder, T., and J. Alexander, 2001, The physical character of subaqueous sedimentary density flows and their deposits: Sedimentology, v. 48, p. 269–299, doi:10.1046/j.1365-3091.2001.00360.x.

Mulder, T., P. P. Razin, and J. C. Faugeres, 2009, Hummocky cross-stratification-like structures in deep-sea turbidites: Upper Cretaceous Basque basins (Western Pyrenees, France): Sedimentology, v. 56, p. 997–1015, doi:10.1111/j.1365-3091.2010.01163.x.

Mulder, T., P. Razin, J. C. Faugeres, and J. Gerard, 2011, Reply to the Discussion by Roger Higgs on "Hummocky cross-stratification-like structures in deep-sea turbidites: Upper Cretaceous Basque basins (Western Pyrenees, France)" by Mulder et al.: Sedimentology, v. 56, p. 997–1015: Sedimentology, v. 58, p. 571–577, doi:10.1111/j.1365-3091.2010.01162.x.

Mutti, E., 1992, Turbidite sandstones: AGIP, Institute of Geology, University of Parma, Milan, Italy, 275 p.

Mutti, E., R. Tinterri, G. Benevelli, D. di Biase, and G. Cavanna, 2003, Deltaic, mixed and turbidite sedimentation of ancient foreland basins: Marine and Petroleum Geology, v. 20, p. 733–755, doi:10.1016/j.marpetgeo.2003.09.001.

Owen, G., M. Moretti, and P. Alfaro, 2011, Recognizing triggers for soft-sediment deformation: Current understanding and future directions: Sedimentary Geology, v. 235, p. 133–140, doi:10.1016/j.sedgeo.2010.12.010.

Pantin, H. M., and M. R. Leeder, 1987, Reverse flow in turbidity currents: The role of internal solitons: Sedimentology, v. 34, p. 1143–1155, doi:10.1111/j.1365-3091.1987.tb00597.x.

Peters, S. E., and D. P. Loss, 2012, Storm and fair-weather wave base: A relevant distinction?: Geology, v. 40, p. 511–514, doi:10.1130/G32791.1.

Phelps, R. M., C. Kerans, R. G. Loucks, R. Da-Gama, J. Jeremiah, and D. Hall, 2013, Oceanographic and eustatic control of carbonate platform evolution and sequence stratigraphy on the Cretaceous (Valanginian-Campanian) passive margin, northern Gulf of Mexico: Sedimentology, v. 62, p. 461–496, doi:10.1111/sed.12062.

Pickering, K. T., and R. N. Hiscott, 1985, Contained (reflected) turbidity currents from the Middle Ordovician Cloridorme Formation, Quebec, Canada: An alternative to the antidune hypothesis: Sedimentology, v. 32, p. 373–394, doi:10.1111/j.1365-3091.1985.tb00518.x.

Pierce, J. D., S. C. Ruppel, H. Rowe, and D. F. Stockli, 2016, Zircon U–Pb geochronology and sources of volcanic ash beds in the Upper Cretaceous Eagle Ford Shale, South Texas: Gulf Coast Association of Geological Societies Journal, v. 5, p. 254–274, <http://gcags.org/Journal/2016.GCAGS.Journal/2016.GCAGS.Journal.v5.15.p253-274.Pierce.et.al.pdf> Last accessed August 2, 2018.

Prave, A. R., and W. L. Duke, 1990, Small-scale hummocky cross-stratification in turbidites; a form of antidune stratification: Sedimentology, v. 37, 531–539, doi:10.1111/j.1365-3091.1990.tb00152.x.

Reading, H. G., and J. D. Collinson, 1996, Clastic coasts, *in* H. G. Reading, ed., Sedimentary environments: Processes, facies and stratigraphy: Blackwell Science, Oxford, U.K., p. 154–258.

Roth, P. H., 1994, Distribution of coccoliths in oceanic sediments, *in* A. Winter and W. G. Siesser, eds., Coccolithophores: Cambridge University Press, U.K., p. 199–218.

Savrda, C. E., and D. J. Bottjer, 1989, Trace-fossil model for reconstructing oxygenation histories of ancient marine bottom waters: Application to Upper Cretaceous Niobrara Formation, Colorado: Palaeogeography, Palaeoclimatology, Palaeoecology, v. 74, p. 49–74, doi:10.1016/0031-0182(89)90019-9.

Shanmugam, G., 2008, Deep-water bottom currents and their deposits, *in* M. C. Rebesco and C. Camerlenghi, eds., Contourites: Elsevier Science, Amsterdam, The Netherlands, p. 59–81, doi:10.1016/S0070-4571(08)10005-X.

Stanley, D. J., 1993, Model for turbidite-to-contourite continuum and multiple process transport in deep marine settings: Examples in the rock record: Sedimentary Geology, v. 82, p. 241–255, doi:10.1016/0037-0738(93)90124-N.

Steinmetz, J. C., 1994, Sedimentation of coccolithophores, *in* A. Winter and W. Siesser, eds., Coccolithophores: Cambridge University Press, U.K., p. 13–37.

Stow, D. A. V., J. C. Faugeres, A. Viana, and E. Gonthier, 1998, Fossil contourites: A critical review: Sedimentary Geology, v. 115, p. 3–31, doi:10.1016/S0037-0738(97)00085-7.

Treviño, R. H., 1988, Facies and depositional environments of the Boquillas Formation, Upper Cretaceous of southwest Texas: M.S. Thesis, University of Texas at Arlington, 135 p.

van der Zwann, G. J., F. J. Jorissen, and H. C. de Stigter, 1990, The depth dependency of planktonic/benthic foraminiferal ratios: Constraints and applications: Marine Geology, v. 95, p. 1–16, doi:10.1016/0025-3227(90)90016-D.

Vink, A., 2004, Calcareous dinoflagellate cysts in South and equatorial Atlantic surface sediments: Diversity, distribution, ecology and potential for paleoenvironmental reconstruction: Marine Micropaleontology, v. 50, p. 43–88, doi:10.1016/S0377-8398(03)00067-7.

Weaver, J. D., and R. E. Jeffcoat, 2009, Carbonate ball and pillow structures: Geological Magazine, v. 115, p. 245–253, doi:10.1017/S0016756800037158.

Wehner, M., R. Gardner, M. M. Tice, M. C. Pope, A. D. Donovan, and T. S. Staerker, 2015, Anoxic, storm dominated inner carbonate ramp deposition of lower Eagle Ford Formation, West

Texas: Proceedings of the 3rd Unconventional Resources Technology Conference (URTeC), San Antonio, Texas, 16 p., doi:10.15530/urtec-2015-2154667.

Williams, J. D., 1963, The petrology and petrography of sediments from the Sigsbee blanket, Yucatan Shelf, Mexico: American Petroleum Institute Project 63, Washington, D.C., and Texas A&M University Department of Oceanography and Meteorology Project 287A, Reference 63–12T, College Station, 60 p.

Ziveri, P., A. T. C. Broerse, J. E. van Hinte, P. Westbroeck, and S. Honjo, 2000a, The fate of coccoliths at 48°N 21°W, northeastern Atlantic: Deep-Sea Research II, v. 47, p. 1853–1875, doi:10.1016/S0967-0645(00)00009-6.

Ziveri, P., A. Rutten, G. J. de Lange, J. Thomson, and C. Corselli, 2000b, Present-day coccolith fluxes recorded in central eastern Mediterranean sediment traps and surface sediments: Palaeogeography, Palaeoclimatology, Palaeoecology, v. 158, p. 175–195, doi:10.1016/S0031-0182(00)00049-3.